

Discovery of Icenticaftor (QBW251), a Cystic Fibrosis Transmembrane Conductance Regulator Potentiator with Clinical Efficacy in Cystic Fibrosis and Chronic Obstructive Pulmonary Disease

Darren Le Grand, Martin Gosling, Urs Baettig, Parmjit Bahra, Kamlesh Bala, Cara Brocklehurst, Emma Budd, Rebecca Butler, Atwood K. Cheung, Hedaythul Choudhury, Stephen P. Collingwood, Brian Cox, Henry Danahay, Lee Edwards, Brian Everatt, Ulrike Glaenzel, Anne-Lise Glotin, Paul Groot-Kormelink, Edward Hall, Julia Hatto, Catherine Howsham, Glyn Hughes, Anna King, Julia Koehler, Swarupa Kulkarni, Megan Lightfoot, Ian Nicholls, Christopher Page, Giles Pergl-Wilson, Mariana Oana Popa, Richard Robinson, David Rowlands, Tom Sharp, Matthew Spendiff, Emily Stanley, Oliver Steward, Roger J. Taylor, Pamela Tranter, Trixie Wagner, Hazel Watson, Gareth Williams, Penny Wright, Alice Young, and David A. Sandham*



Cite This: *J. Med. Chem.* 2021, 64, 7241–7260



Read Online

ACCESS |



Metrics & More

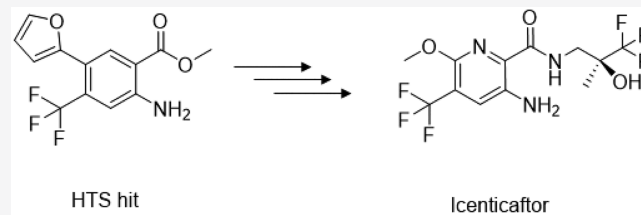


Article Recommendations



Supporting Information

ABSTRACT: Mutations in the cystic fibrosis transmembrane conductance regulator (CFTR) ion channel are established as the primary causative factor in the devastating lung disease cystic fibrosis (CF). More recently, cigarette smoke exposure has been shown to be associated with dysfunctional airway epithelial ion transport, suggesting a role for CFTR in the pathogenesis of chronic obstructive pulmonary disease (COPD). Here, the identification and characterization of a high throughput screening hit **6** as a potentiator of mutant human F508del and wild-type CFTR channels is reported. The design, synthesis, and biological evaluation of compounds **7–33** to establish structure–activity relationships of the scaffold are described, leading to the identification of clinical development compound icenticaftor (QBW251) **33**, which has subsequently progressed to deliver two positive clinical proofs of concept in patients with CF and COPD and is now being further developed as a novel therapeutic approach for COPD patients.



INTRODUCTION

Cystic fibrosis (CF) is the most prevalent life-threatening Mendelian disorder in Caucasian populations.¹ CF arises from mutations of the gene for the cystic fibrosis transmembrane conductance regulator (CFTR) protein.² The CFTR ion channel orchestrates gating of chloride and bicarbonate ions across epithelial cell membranes in various tissues, including the lung, pancreas, intestine, reproductive tract, and sweat glands. While CF is a systemic disorder, the primary mortality derives from reduced CFTR activity in the airways. Subsequent acidification³ and dehydration leads to accumulation of a viscous mucus layer, occluding the airways and trapping bacteria, leading to infections, reduced lung function, and ultimately, respiratory failure. The most common CFTR mutation, F508del (Class II, found in 90% of CF patients), impairs folding of the CFTR protein (a Class II trafficking defect), resulting in a reduced amount of channel present at the plasma membrane. With the G551D mutation (class III), the

amount of protein at the membrane is unaffected, but its open probability (P_o) is reduced, also resulting in a reduced channel gating.⁴ Thus, to address the underlying causes of CF, two distinct CFTR modulators are required: correctors to increase CFTR levels at the plasma membrane and potentiators to enable effective opening of the channel.⁴

Significant progress in the CFTR modulator field was initiated by Vertex with the 2011 registration of the potentiator ivacaftor **1**⁵ (Figure 1) for patients with the G551D mutation followed by the 2015 approval of the fixed dose combination of ivacaftor with the corrector lumacaftor (Orkambi) for homozygous

Received: February 24, 2021

Published: May 24, 2021



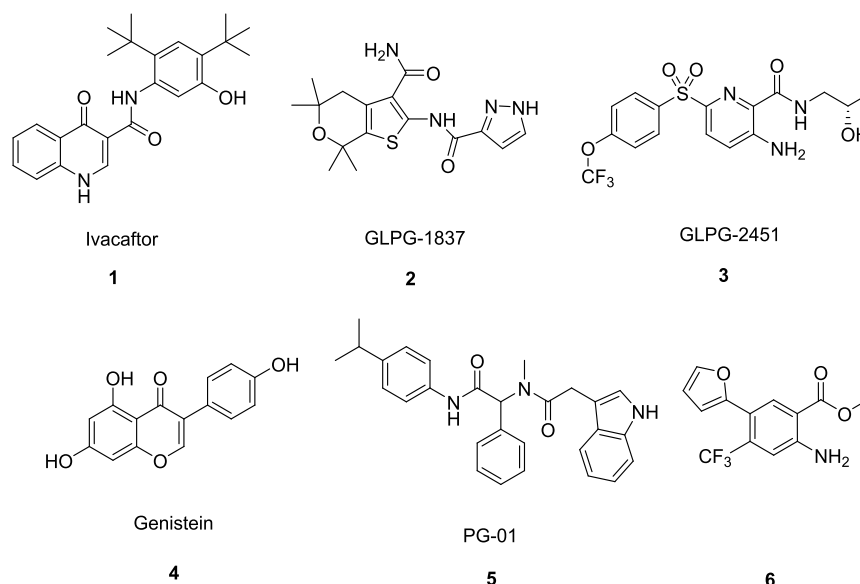


Figure 1. Selected reported CFTR potentiators 1–5 and high throughput screening hit 6.

F508del CF patients.⁶ Most recently, the addition of a second site CFTR corrector agent to a potentiator–corrector combination was shown to give improvement in lung function in both hetero- and homozygous F508del CF patients, leading to the 2019 US registration of the ivacaftor–tezacaftor–elxacaftor (Trikafta) fixed dose combination.⁷ Further CFTR potentiator–corrector combinations are in development from AbbVie, with the clinical stage potentiators GLPG1837 **2**⁸ and GLPG2451 **3**⁹ (Figure 1) disclosed, and the broader field of CFTR potentiator discovery has also been recently reviewed.¹⁰

Chronic obstructive pulmonary disease (COPD) is anticipated to shortly become the third leading cause of death globally.¹¹ COPD is characterized by persistent airflow obstruction¹² with cigarette smoke exposure recognized as the primary risk factor.¹³ Airflow limitation is associated with all COPD patients; however, the disease is heterogeneous, with variable phenotypes ranging from chronic bronchitis (CB) to emphysema.¹³ Small airway disease exhibits increased numbers of goblet cells and mucus plugging with associated smooth muscle hyperplasia, airway fibrosis, and increased inflammation.^{14,15} Excess mucus secretion is believed to play an important role in COPD pathogenesis^{16,17} and is associated with progression of the disease.^{18–21}

Smoking-induced acquired dysregulation of CFTR may contribute to COPD pathogenesis. *In vitro*, cigarette smoke condensate induced CFTR dysfunction results in reduction of airway surface liquid (ASL) and decreased mucociliary transport (MCT).^{22–25} In clinical studies, cigarette smokers and COPD patients show reduced CFTR function both in upper and lower airways as well as systemically, which is associated with CB.^{26–29} Collectively, the importance of mucus hypersecretion, chronic airway inflammation, and recurrent infections in both COPD and CF suggests that acquired CFTR dysfunction may contribute to the pathophysiology of COPD, particularly in COPD patients with CB.

Preclinical data with the CFTR potentiator ivacaftor indicates restoration of CFTR-dependent ion transport in cigarette smoke-exposed epithelial cells and improvement of the downstream effects of epithelial function.²⁵ Preclinical data with the phosphodiesterase 4 inhibitor roflumilast (which

reduces the risk of exacerbations in COPD patients with CB) suggests that CFTR activation may contribute to the drug's mechanism of action via phosphorylation of the CFTR regulatory domain and partial restoration of CFTR-dependent ion transport in cigarette smoke-exposed epithelial cells.³⁰ Prior to the clinical data in COPD reported herein (*vide infra*), only one small pilot study of two weeks in duration with ivacaftor in COPD patients revealed nonstatistically significant improvements in sweat chloride, nasal potential difference, and symptom scores compared with placebo.³¹

Here, the identification and characterization of a high throughput screening hit **6** as a potentiator of human F508del and wild-type CFTR channels is reported. The design, synthesis, and biological evaluation of compounds **7–33** to establish structure–activity relationships (SAR) of the scaffold are described, leading to the identification of clinical development compound icentricaftor (QBW251) **33**, which has subsequently progressed to deliver two positive clinical proofs of concept in patients with CF and COPD and is now being further developed as a novel therapeutic approach for COPD.

RESULTS AND DISCUSSION

At the outset of CFTR modulator drug discovery activities at Novartis in the mid-2000s, CF was envisaged as the primary indication, and a screening strategy based around the most prevalent CFTR F508del mutation was devised with the known CFTR potentiators genistein **4**³² and PG-01 **5**³³ (Figure 1) initially used as reference compounds. A high throughput screen (approximately 1 million compounds) was conducted using CFTR F508del stably expressed in human CHO-K1 cells, determining changes in membrane potential due to CFTR-mediated ion efflux in response to the adenylate cyclase activator forskolin. A fluorophore dye partitions across the cell membrane according to the resting potential; upon efflux of Cl[−] mediated by CFTR (and consequent depolarization of the cells), the dye accumulates inside the cell, where it binds to intracellular proteins, and the increased fluorescence signal is measured using a fluorimetric imaging plate reader (FLIPR).³⁴ The assay was also temperature corrected to facilitate membrane insertion of the channel.³⁵ This FLIPR assay proved to be a robust and cost-

effective primary screen which identified multiple hits that were further characterized via automated 384 well planar patch clamp electrophysiology (IonWorks Quattro), using the same CFTR F508del CHO cell line.

A further, higher fidelity, lower throughput characterization of ion transport properties was also performed, measuring changes in short circuit current (ΔI_{sc}) in Ussings chambers with CFTR F508del expressed in Fisher Rat Thyroid (FRT) cells, in parallel with the same determination on wild-type (WT) CFTR expressed in FRT cells. An acceptable correlation between electrophysiology and ion transport assays was found on a test set of validated hit compounds (Figure 2), providing confidence for use of the Quattro assay as the primary screen for subsequent compound optimization.

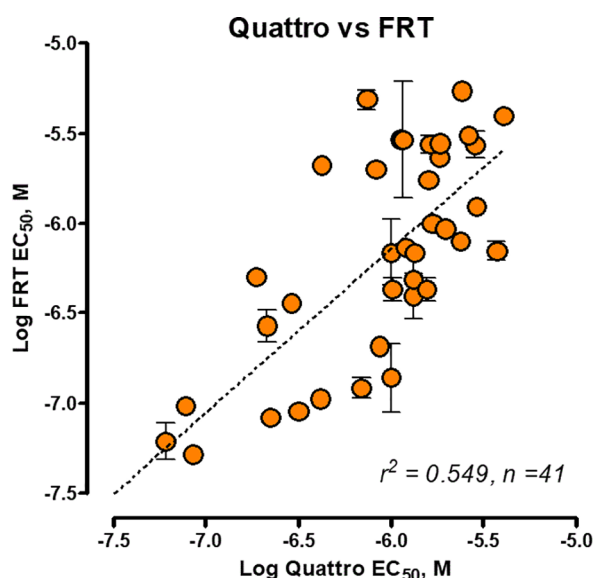


Figure 2. Correlation of automated electrophysiology (Quattro) with ion transport (FRT) assay potency for F508del CFTR.

With this paradigm, the anthranilate derivative **6** was identified as one of a number of validated hits with superior potency to genistein and PG-01 (Table 1) in F508del CFTR and evidence for potentiation of WT CFTR channels.

Additional profiling to evaluate the general pharmacology of compound **6** showed it to be selective for the potentiation of CFTR against a broad panel of 46 G-protein coupled receptor, enzyme, transporter, and ion channels (including hERG) as well as 20 kinase targets with no observed inhibition >50% at 10 μ M concentration (Supporting Information Tables S2 and S3). In addition, a negative result was obtained in a mini-Ames test, in line with the reported nonmutagenicity of other anthranilates.³⁶ Initial assessment of the biopharmaceutical properties of compound **6** (Table 2) showed the impact of the high lipophilicity on solubility and free fraction, with thermodynamic

solubility measurements <0.001 g/L and equilibrium dialysis experiments using rat plasma confirming a high level of plasma protein binding at 99.5%. High *in vitro* clearance in the rat microsomal assay was confirmed *in vivo*, with a short intravenous mean residence time (MRT) of less than 15 min, reflecting a moderate level of plasma clearance combined with a small volume of distribution. The high levels of nonspecific binding to plasma proteins reduced the scope to achieve unbound drug concentrations in plasma consistent with the free drug hypothesis without substantially increasing the affinity for the target or the dose administered. Despite this unfavorable biopharmaceutical profile, the overall lipophilic ligand efficiency (LLE)³⁷ of 3.9 (Table 2) based on the Quattro assay potency, combined with the low molecular weight represented an acceptable starting point for hit-to-lead chemistry. These considerations prompted exploration of opportunities to achieve the desired drug exposure metric through a combination of increasing binding affinity for CFTR and reducing lipophilicity. Such an approach by definition focused on increasing the LLE of the compound class while minimizing liver microsomal clearance. Furthermore, in the absence of an available animal PK–PD or disease model for CF, maximization of free drug exposure was set as a key objective for identification of a development candidate.

To establish the minimum pharmacophore for CFTR potentiator activity and identify a lead compound with optimal ligand efficiency, the scaffold was simplified to identify the key groups required for binding site recognition. Initially retaining the methyl ester, the furan ring of **6** with its known potential for reactive metabolite formation³⁸ was first targeted (Table 3). Excising the furan to afford the 4-trifluoromethyl substituted anthranilate ester **7** gave a drop in potency of 23-fold but with similar efficacy to **6**. Further pruning of the scaffold to the unsubstituted anthranilate **8** abolished all activity, and exploration of a further range of substituents at the 5-position gave either inactive or minimally active compounds (data not shown), leading to retention of the trifluoromethyl group in all later analogues. The potencies of the iodo synthetic intermediate **9** and 5- and 6-membered aromatic heterocycles **10** and **11** derived from it, together with the saturated heterocycle **12**, established from the outset the broad tolerance of this position to a range of substituents. There was little improvement in rat microsomal clearance with these early analogues, although solubility was markedly improved with the heterocycles **10**–**12**. As anticipated, solubility was also improved by insertion of a nitrogen atom to give the picolinate analogue **13**, at the expense of >50 fold potency loss.

While the ester group of **6** itself was hydrolytically stable in plasma, the corresponding acid **14** was readily prepared by basic hydrolysis and found to be >50 fold less potent than **6** (Table 4). To avoid routine screening of new compounds for plasma stability, replacement of the ester group with amides was next studied (Table 4). With an emphasis on identifying compounds

Table 1. CFTR Assay Characterization of HTS Hit **6** in Comparison to Genistein **4** and PG-01 **5**

compound ^a	CFTR F508del CHO membrane potential EC ₅₀ (μ M) (% efficacy ^b)	CFTR F508del CHO Quattro EC ₅₀ (μ M) (% efficacy ^b)	CFTR F508del FRT ion transport EC ₅₀ (μ M) (% efficacy ^b)	CFTR WT FRT ion transport EC ₅₀ (μ M) (% efficacy ^b)
4	8.20 (83)	8.48 (88)	6.17 (54)	14.2 μ M (138)
5	0.39 (100)	1.25 (100)	0.260 (100)	0.99 μ M (100)
6	0.92 (154)	0.078 (93)	0.180 (100)	30 μ M (206) ^c

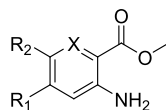
^aData is mean of $n \geq 2$. ^bEfficacy relative to E_{max} of PG-01 set at 100%. ^cEfficacy at a single concentration of 30 μ M.

Table 2. Physicochemical, Biopharmaceutical, and Pharmacokinetic Properties of Compound 6

MW	clogP	LLE	solubility pH 6.8 (g/L)	PAMPA ^a permeability logPe pH 6.8	rat Cl _{int} ^c (μL/min/mg)	rat PPB ^b (%)	rat in vivo PK ^c			
							Cl (mL/min/kg)	V _{dss} (L/kg)	MRT (hr)	F _{po} (%)
285	3.2	3.9	<0.001	−4.5	351	99.5	30	0.4	0.2	15

^aParallel artificial membrane permeability assay. ^bPlasma protein binding determined by equilibrium dialysis. ^cI.v. dose 0.5 mg/kg, p.o. dose 5 mg/kg (suspension), vehicle details in Table S4 (Supporting Information).

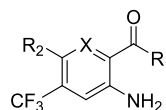
Table 3. Initial Optimization of HTS Hit 6 Retaining the Methyl Ester



compound	R ₁	R ₂	X	dF508 Quattro EC ₅₀ (μM) ^a (% efficacy ^b)	rat Cl _{int} ^c (μL/min/mg)	solubility pH 6.8 (g/L)	LLE
6	CF ₃	2-furan	CH	0.078 (98)	351	<0.001	3.9
7	CF ₃	H	CH	3.78 (72)	nd ^d	<0.001	2.9
8	H	H	CH	>30 (0)	nd	nd	<2.6
9	CF ₃	I	CH	0.362 (104)	342	0.002	3.5
10	CF ₃	2-oxazole	CH	0.240 (92)	239	0.036	3.8
11	CF ₃	3-pyridine	CH	0.329 (100)	217	0.056	3.2
12	CF ₃	(±)-2-tetrahydrofuran	CH	0.462 (90)	185	0.006	3.3
13	CF ₃	2-furan	N	5.31 (72)	>700	0.011	2.4

^aData is mean of $n \geq 2$ determinations. ^bEfficacy relative to PG-01 maximal effect. ^cMicrosomal clearance with NADPH cofactor representing CYP mediated metabolism. ^dnd: not determined.

Table 4. Replacements for the Methyl Ester of HTS Hit 6



compound	R ₁	R ₂	X	dF508 Quattro EC ₅₀ (μM) ^a (% efficacy ^b)	rat Cl _{int} ^c (μL/min/mg)	solubility pH 6.8 (g/L)	LLE
6	OMe	2-furan	CH	0.078 (98)	351	<0.001	3.9
14	OH	2-furan	CH	5.83 (63)	201	nd ^d	2.4
15	NHMe	2-furan	CH	1.86 (83)	205	0.013	3.1
16	NMe ₂	2-furan	CH	>30 (37)	nd	nd	<1.9
17	NHMe	Br	N	0.250 (97)	100	nd	4.5
18	NH(CH ₂) ₂ CF ₃	Br	N	0.040 (132)	55.8	0.049	4.5
19	(±)-NHCH ₂ CH(OH)Me	Br	N	0.070 (79)	37.7	0.12	5.0
20	(S)-NHCH ₂ CH(OH)(CF ₃)	Br	N	0.023 (102)	23	0.290	5.2
21	(R)-NHCH ₂ CH(OH)(CF ₃)	Br	N	0.009 (100)	37.1	0.177	5.6

^aData are mean of $n \geq 2$ determinations. ^bEfficacy relative to PG-01 maximal effect. ^cMicrosomal clearance with NADPH cofactor representing CYP mediated metabolism. ^dnd: not determined.

Table 5. Rat in Vivo Pharmacokinetic and in Vitro Protein Binding Profiles in Plasma of Selected Compounds

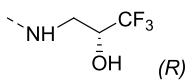
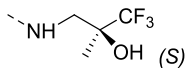
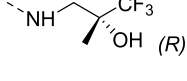
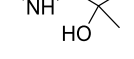
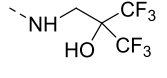
compound ^a	F _{po} (%)	AUC _{last} (nmol/h/L)	C _{max} (nM)	C _{max} (nM) [unbound]	CL (mL/min/kg)	V _{dss} (L/kg)	MRT (h)	PPB (% rat) ^b	PPB (% human) ^b
21	32	652	271	nd ^c	53	3.2	1.0	nd	nd
22	114	7739	634	25	17	6.5	6.4	96.9	97.5
29	75	5929	595	11	15	6.4	7.2	98.1	98.6
33	90	20 635	1364	132	5	3.0	10.2	90.3	92.3 ^d

^aDoses i.v. 1 mg/kg (except 21 0.5 mg/kg) and p.o. 3 mg/kg (suspension); vehicle details in Table S4 (Supporting Information). ^bPlasma protein binding determined by equilibrium dialysis. ^cnd: not determined. ^dDetermined with [¹⁴C]-33 (synthesis to be reported separately).

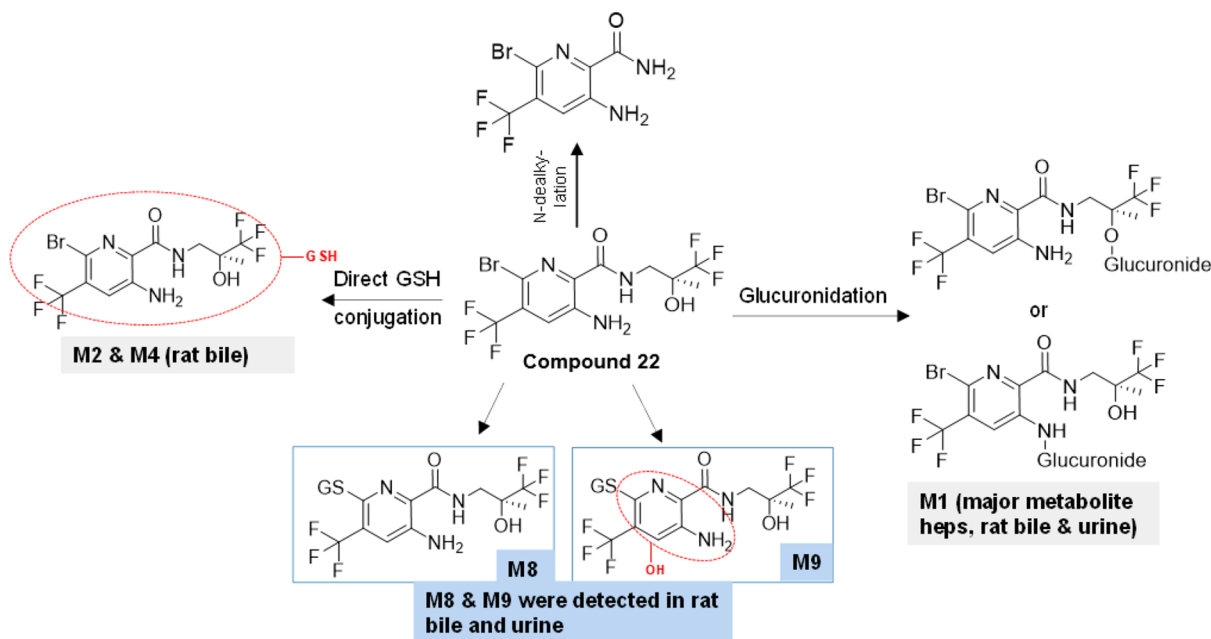
having improved lipophilic ligand efficiency, simple amide derivatives of both the anthranilate and picolinate scaffolds were explored. Synthesis of the *N*-methyl and *N*-dimethyl amide derivatives 15 and 16 clearly indicated a preference for the secondary amide 15. The retention of some activity in the iodo ester analogue 9 (*vide supra*) led to consideration of bromine as a

less reactive alternative, together with the combination of ester replacement and the potentially improved properties of the picolinate core. Thus, a key advance was made with 6-bromo picolinate *N*-methyl amide 17, suggesting divergence from the SAR of the anthranilate scaffold. With these data available, a library of commercially available primary amines was employed

Table 6. Lead Optimization of 21 to Incorporate a Tertiary Alcohol

compound	R	dF508 Quattro		solubility pH 6.8 (g/L)	LLE
		EC ₅₀ (μM) ^a (% efficacy) ^b	rat Cl _{int} ^c (μL/min/mg)		
21		0.009 (100)	37.1	0.177	5.6
22		0.015 (107)	5.3	0.140	5.3
23		0.030 (91)	23	0.160	5.0
24		0.077 (101)	<25	0.280	4.9
25		0.010 (117)	nd ^d	0.003	4.9

^aData are mean of $n \geq 2$ determinations. ^bEfficacy relative to PG-01 maximal effect. ^cMicrosomal clearance with NADPH cofactor representing CYP mediated metabolism. ^dnd: not determined.

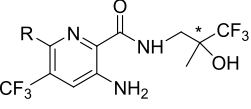
Figure 3. *In vivo* metabolism of compound 22 in the rat.

to elaborate 17, resulting in identification of the first sub-100 nM potency potentiators 18–20, with some improvement in microsomal clearance compared to earlier compounds. Replacement of the methyl group of 19 with trifluoromethyl in enantiomers 20 and 21 gave a 10-fold improvement in activity over the *N*-methyl amide 17 and a further reduction in the microsomal clearance, with the (*R*) enantiomer 21 being marginally more active.

The oral pharmacokinetic profile of 21 was established in Sprague–Dawley rats (Table 5). Despite the reduced intrinsic

clearance *in vitro*, 21 showed a high clearance rate *in vivo* that limited its oral bioavailability and overall exposure with a short mean residence time of 1 h. Although metabolism of 21 was not characterized, it was speculated that the secondary alcohol could be cleared through direct glucuronidation of the hydroxyl group, limiting the compounds systemic exposure. In addition, possible metabolic oxidation of the secondary alcohol to the trifluoromethyl ketone derivative was considered, which might then undergo reversible covalent interactions with nucleophilic amino acid side chains that could potentially lead to

Table 7. Final Optimization of Advanced Lead 22



compound	R	stereochemistry ^a	dF508 Quattro EC ₅₀ (μM) ^b (% efficacy ^c)	rat Cl _{int} ^d (μL/min/mg)	solubility pH 6.8 (g/L)	LLE
22	Br	(S)	0.015 (107)	5.3	0.140	5.3
26	H	(±)	0.229 (78)	<25	nd ^e	4.7
27	Me	(±)	0.240 (99)	73.8	nd	4.5
28a	Et	ent-1	0.008 (100)	85.6	0.091	5.4
28b	Et	ent-2	0.043 (101)	nd	nd	4.2
29	CF ₃	(S)	0.009 (113)	7.38	0.082	5.5
30a	MeNH	ent-1	0.276 (91)	<25	0.013	4.0
30b	MeNH	ent-2	0.111 (95)	nd	nd	4.3
31a	Me ₂ N	ent-1	0.020 (89)	102	0.165	4.9
31b	Me ₂ N	ent-2	0.046 (93)	114	nd	4.5
32	EtO	(S)	0.015 (116)	39	0.06	5.5
33	MeO	(S)	0.047 (96)	11	0.237	5.2

^aent-1 and ent-2 denote single enantiomers of undetermined stereochemistry reported in order of preparative chiral SFC elution. ^bData are mean of $n \geq 2$ determinations. ^cEfficacy relative to PG-01 maximal effect. ^dMicrosomal clearance with NADPH cofactor representing CYP mediated metabolism. ^end: not determined.

Table 8. Further CFTR Ion Transport Characterization of 22 and Ivacaftor 33 in Comparison to Ivacaftor 1

compound ^a	CFTR F508del FRT EC ₅₀ (μM) (% efficacy) ^b	CFTR G551D FRT EC ₅₀ (μM) (% efficacy) ^b	CFTR WT FRT EC ₅₀ (μM) (% efficacy) ^b	CF F508del primary HBEC ^c EC ₅₀ (μM) (% efficacy) ^d	WT primary HBEC ^c EC ₅₀ (μM) (% efficacy) ^d
1	0.049 ± 0.019 (83)	0.131 ± 0.073 (107)	0.070 ± 0.020 (122)	0.068 ± 0.026 (100)	0.034 ± 0.017 (100)
22	0.018 ± 0.006 (106)	0.150 ± 0.044 (67)	0.043 ± 0.041 (140)	0.025 ± 0.012 (113)	nd ^e
33	0.079 ± 0.052 (92)	0.497 ± 0.198 (40)	0.113 ± 0.045 (79)	0.039 ± 0.022 (84)	0.072 ± 0.045 (87)

^aData is mean of $n \geq 3$ determinations ± SD. ^bEfficacy relative to PG-01 set at 100%. ^c $n = 3$ donors. ^dEfficacy relative to ivacaftor set at 100%. ^eNot determined.

idiosyncratic toxicity.³⁹ To address these concerns, a tertiary alcohol was introduced to hinder access to the hydroxy group while at the same time prevent its oxidation to the ketone (Table 6).

In this case, the (S)-enantiomer 22 (absolute configuration confirmed via single crystal X-ray crystallography analysis, Supporting Information Figure S1) was slightly more potent and also showed lower microsomal clearance than the (R)-enantiomer 23, with the rat pharmacokinetic profile of 22 (Table 5) translating into reduced *in vivo* clearance and improved oral exposure, together with a higher free fraction in both rat and human plasma. The introduction of an asymmetric carbon in compounds 20–23 without a large enantiomeric preference for CFTR potentiator activity led to exploration of alternative achiral analogues. The 2-hydroxy-2-methylpropyl amide 24 demonstrated a fivefold reduction in potency, indicating a requirement for the more lipophilic trifluoromethyl group at this position. While replacing both methyl groups with trifluoromethyls provided the potent derivative 25, the higher lipophilicity and poor solubility (pH 6.8 buffer 0.003 g/L) was inconsistent with the goal of improving lipophilic efficiency and biopharmaceutical properties.

Mindful of the potential for nucleophilic aromatic substitution of the 6-bromo group of compound 22 *in vivo*, leading to covalent adduct formation and the potential for idiosyncratic toxicity,³⁹ *in vitro* incubation studies with rat and human liver microsomes in the presence of NADPH and glutathione (GSH) to search for evidence of adduct formation were conducted. After incubation in both rat and human liver microsomes for 1 h, no evidence of direct GSH adduct formation was detected by LC-MS (data not shown). In a follow up *in vivo* study, bile was

cannulated from Sprague–Dawley rats dosed intravenously with 1 mg/kg of compound 22. Contrary to *in vitro* findings, LC-MS analysis of the bile collected over 24 h indicated the presence of glutathione adducts M8 and M9 caused by displacement of the bromine (Figure 3).

Further optimization was thus focused on replacement of the 6-bromo moiety (Table 7; compounds 28, 30, and 31 were separated by preparative chiral SFC with enantiomer absolute configurations not determined). Consistent with the early analogue 7, potency was reduced on deletion of bromine in 26. While methyl analogue 27 showed a similar potency reduction, ethyl analogue 28a delivered comparable potency to 22 at the expense of higher clearance. The corresponding trifluoromethyl analogue 29 gave an increase in potency, combined with a favorable *in vitro* clearance profile which translated *in vivo* to low clearance and good exposure in a rat PK study, although this was associated with a decrease in unbound fraction compared to 22 (Table 5). Replacing the bromine with *N*-methyl, compound 30, and *N,N*-dimethylamino, compound 31, gave a stepwise increase in potency with single enantiomer 31a having similar activity to compound 22, confirming that a hydrophobic interaction at this position was governing affinity for the channel, in preference to modulation of the electronic properties of the aromatic ring. Concordant with this hypothesis, the ethoxy analogue 32 further improved the potency, but again at the expense of metabolic stability. The methoxy substituted compound 33, while not as potent as the trifluoromethyl substituted compound 29, also provided an attractive replacement for the bromine group, showing good metabolic stability. Follow up *in vivo* pharmacokinetic profiling in the rat (Table 5) indicated lower clearance, higher exposure, and a

longer MRT in comparison to compounds **22** and **29** and notably an enhanced free fraction in both rat and human plasma compared to trifluoromethyl analogue **29**.

Compounds **22** and **33** were next further profiled for their CFTR potentiator driven ion transport effects in Ussings chamber experiments, in comparison to ivacaftor/VX770 **1** as a reference standard (Table 8).

First, using F508del, G551D (as an example of a Class III gating mutation) or WT CFTR expressed in FRT cells, the effects of compounds on ΔI_{sc} in the presence of submaximal forskolin stimulation were determined. For the F508del studies, data are reported from temperature corrected experiments. As shown in Table 5, comparable potencies and efficacies were found for all three compounds against WT and F508del CFTR, whereas ivacaftor was more efficacious against G551D CFTR. Next, studies were conducted using the most physiologically relevant available assay with cultured primary human bronchial epithelial cells (HBEC) obtained from healthy (i.e. WT) donors and temperature corrected homozygous F508del CF HBECs. In this assay, amiloride was initially applied to block the ENaC current.⁴⁰ Secondly, potentiation of ΔI_{sc} was measured in response to forskolin, which stimulates adenylate cyclase, leading to protein kinase A mediated CFTR activation.⁴¹ Thirdly, increasing concentrations of the test compound were added; then, at the end of the experiment, the CFTR mediated current was blocked by CFTR inhibitor 172.⁴² A representative raw data trace for WT CFTR is shown in Figure 4.

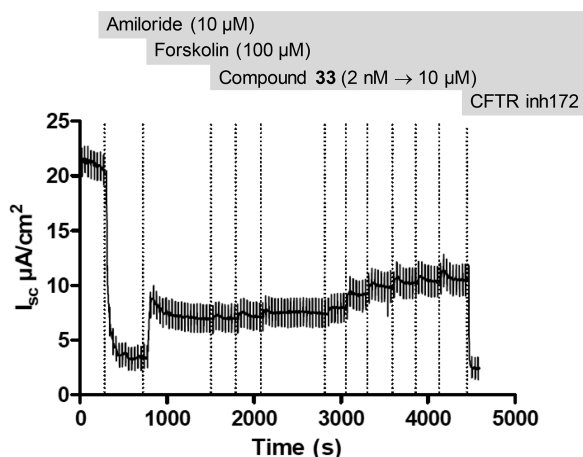


Figure 4. Representative raw data trace from a WT CFTR HBEC ion transport experiment.

Given the equivalent potencies of **22** and **33** in CFTR HBEC assays and similar, clean off-target profiles in a broad safety pharmacology assay panel, both compounds were advanced into

a two-week exploratory toxicology study in rats. Compound **22** was dosed at 10 and 100 mg/kg, with animals in the 100 mg/kg group requiring euthanization after 2 days' dosing. The compound was tolerated at the lower dose for the duration of the study, where mild decreases in all leukocyte subsets were observed, together with bone marrow hypocellularity, corresponding to a No Observable Adverse Effect Level (NOAEL) of <10 mg/kg. In contrast, compound **33** was tolerated at 100 mg/kg, and a NOAEL of 10 mg/kg was identified, with comparable exposures of both compounds determined in toxicokinetic analyses (Supporting Information Table S5). It is not known whether the *in vivo* GSH adduct formation found for **22** (*vide supra*) contributed directly to the observed toxicology of the compound. With these data in hand, **33** was then prioritized as a development candidate. In higher species *in vivo* PK studies (Table 9), increased clearance compared to the rat was found. *In vivo* clearance in the dog was close to liver blood flow in the dog and approximately 50% of liver blood flow in the monkey.⁴³

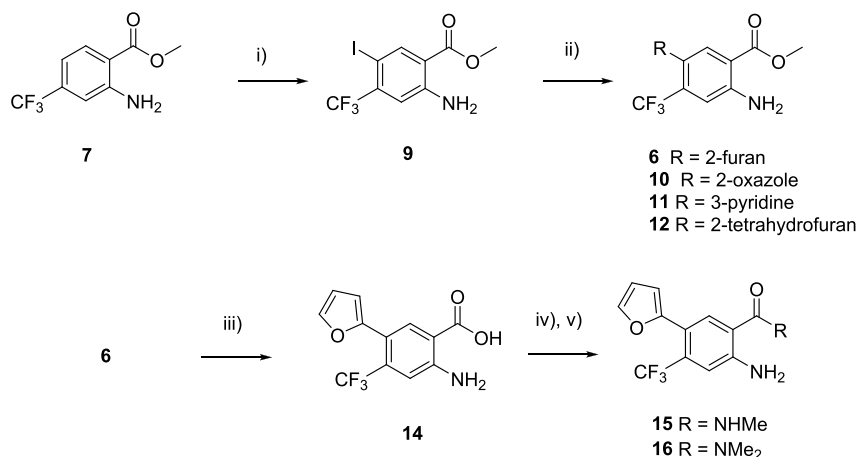
Following further GLP toxicology studies in rats and monkeys, **33** was advanced into a healthy volunteer Phase I study,⁴⁴ where the compound was found to be safe and well-tolerated up to 750 mg bid in a multiple ascending dose study. In a proof of concept (PoC) clinical study for CF, a cohort of patients with CFTR Class III and IV mutations (S549N, R117H, D1152H, R334W, R352Q, and R347H) where channel is present at the membrane was treated with **33** for 14 days at 150 and 450 mg bid doses. The study results showed evidence of CFTR target engagement through a reduction in sweat chloride as well as clinically meaningful improvement in lung function in comparison to placebo. In contrast, a cohort of patients with F508del mutation treated with **33** (450 mg bid) showed no reduction in sweat chloride or improvement in lung function, consistent with prior clinical data with ivacaftor in subjects with the same mutation⁴⁵ and confirming that combination with CFTR correctors is required for this patient group.

In parallel with the CF clinical study, a further PoC study was also initiated in moderate to severe COPD patients with chronic bronchitis, who were treated with **33** at a dose of 300 mg bid for 28 days, on top of standard of care.⁴⁶ In comparison to placebo, **33** showed significant improvements in lung function, together with a reduction in sweat chloride. The systemic anti-inflammatory effect of **33** was supported by the observation of a significant reduction in the qualified prognostic COPD biomarker fibrinogen,⁴⁷ and an exploratory analysis indicated a trend to reduction in sputum bacterial colonization, which may arise from increased mucociliary clearance. Following the COPD PoC data, compound **33** (Novartis code NVP-QBW251; INN icenticaftor) was progressed into a Phase 2b dose range finding study in moderate-to-severe COPD patients with chronic bronchitis, which is currently ongoing.⁴⁸

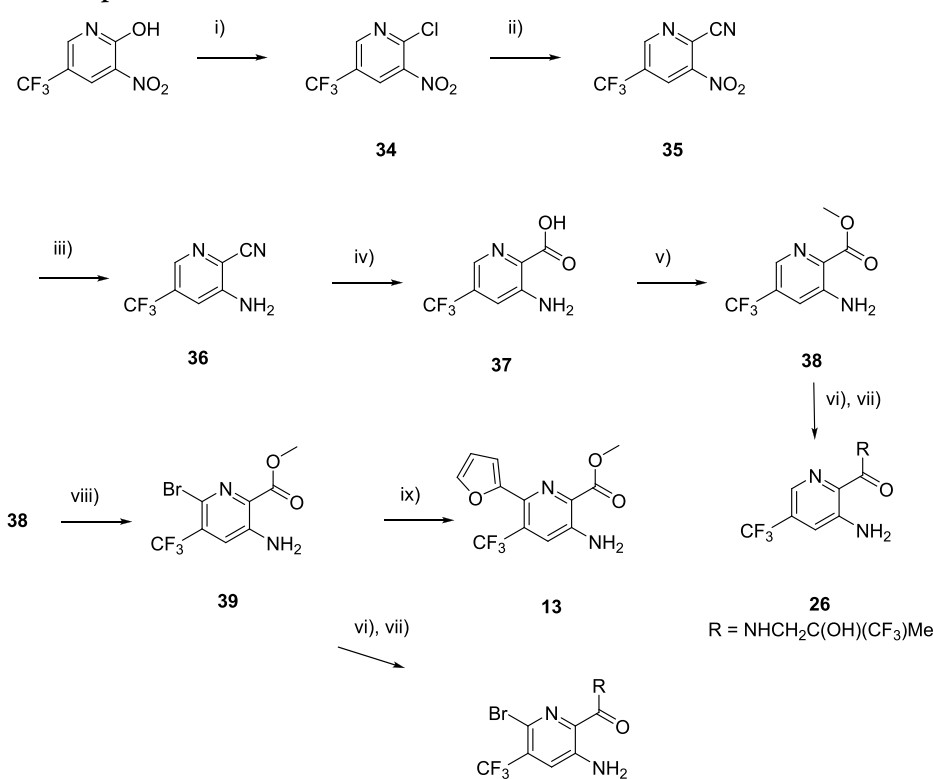
Table 9. Higher Species *in Vivo* Pharmacokinetic Characterization of **33**

species	F_{po} (%)	AUC_{last} (nmol/h/L)	C_{max} (nM)	$C_{max, free}$ (nM)	Cl_{plasma} (mL/min/kg)	Cl_{blood}^d (mL/min/kg)	$V_{d,ss}$ (L/kg)	MRT (h)	PPB (%) ^e
dog ^a	146	8670	1952	102	29	41	7.5	4.4	94.8
monkey ^b	26	6780	2303	276	18	20.2	3.5	3.3	88.0

^aI.v. dose 0.46 mg/kg; p.o. dose 3 mg/kg. ^bI.v. dose 0.1 mg/kg; p.o. dose 10 mg/kg. ^cDetermined by equilibrium dialysis with [¹⁴C]-**33**. ^dDerived from blood/plasma ratios of 0.708 and 0.89 for dog and monkey, respectively.

Scheme 1. Synthesis of Compounds 6, 10–12, 15, and 16^a

^aReagents and conditions; (i) Ag₂SO₄, I₂, MeOH, rt, 18%; (ii) **6**: tri-*n*-butyl-2-furylstannane, Pd(PPh₃)₄, 1,4-dioxane, reflux, 62%; **10**: 2-(tri-*n*-butylstannyl)oxazole, Pd(PPh₃)₄, 1,4-dioxane, reflux, 34%; **11**: [Pd(dppf)Cl₂]₂, 3-pyridineboronic acid, Na₂CO₃, DME, 100°C, μ W, 65%; **12**: compound **6**, ethanol, H-Cube (RaNi CatCart), 70°C, 70 bar, 25%; (iii) 2M NaOH, ethanol, reflux 1 h; 99%; (iv) pyridine/MeCN, triphosgene/DCM, reflux, 71%; (v) **15**: methylamine (40% aq), THF, RT, 45%; **16**: dimethylamine, DMF, RT, 13%.

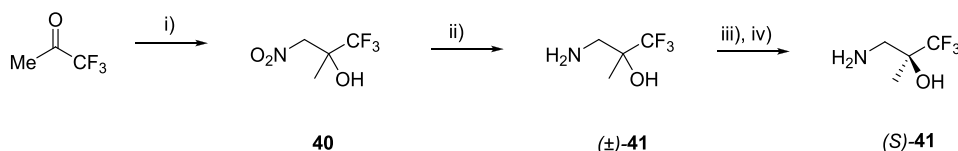
Scheme 2. Synthesis of Compounds 17–26^a

17-25
R as defined in Tables 4, 6 and 7

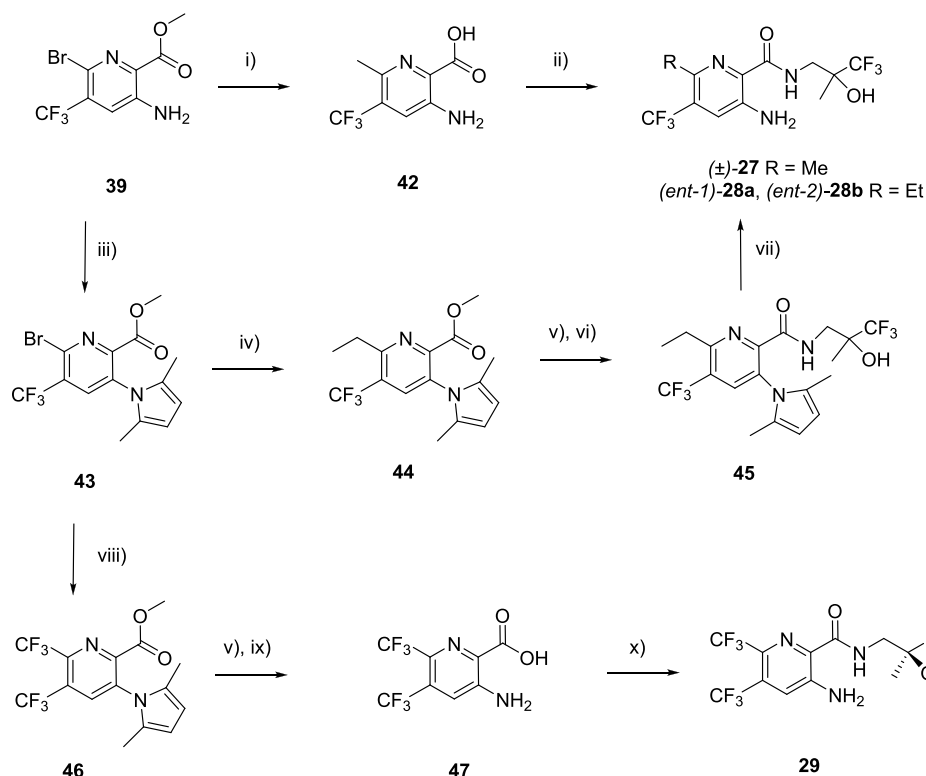
^aReagents and conditions: (i) POCl₃, DMF, 110°C, 85%; (ii) CuCN, NMP, 175°C, 42%; (iii) SnCl₂, EtOH, reflux, 45%; (iv) Conc HCl, reflux, 89%; (v) SOCl₂, MeOH, reflux, 89%; (vi) aq NaOH, MeOH, RT, 91–94%; (vii) primary amine, HATU, *N*-methylmorpholine, DMF, RT, 36–90%; (viii) Br₂, AcOH/H₂SO₄, RT, 67%; (ix) tri-*n*-butyl-2-furylstannane, Pd(PPh₃)₄, 1,4-dioxane, reflux, 57%.

Synthesis. Synthetic routes to compounds **6**–**33** are depicted in Schemes 1–5. Anthranilate compounds **6** and **10**–**12** were synthesized according to Scheme 1, with compound **8** being commercially available. Silver catalyzed iodination of commercially available 4-trifluoromethyl anthra-

nilate ester **7** afforded the iodo compound **9**, which readily reacted with boronate or trialkyltin derived heterocycles under Suzuki or Stille cross coupling conditions to afford the corresponding arylated derivatives **6** and **10**–**12**. Saponification of the ester in **6** followed by triphosgene treatment afforded an

Scheme 3. Synthesis of Compound 41^a

^aReagents and conditions: (i) MeNO₂, aq LiOH, MgSO₄, cetyltrimethylammonium chloride RT, 95%; (ii) H₂, Pd/C, then HCl-EtOH, 97%; (iii) (+)-tartaric acid, EtOH-H₂O, RT, 23% (97.4% ee); (iv) SCX-2 ion exchange cartridge, MeOH-NH₃, RT, 80%.

Scheme 4. Synthesis of Compounds 27–29^a

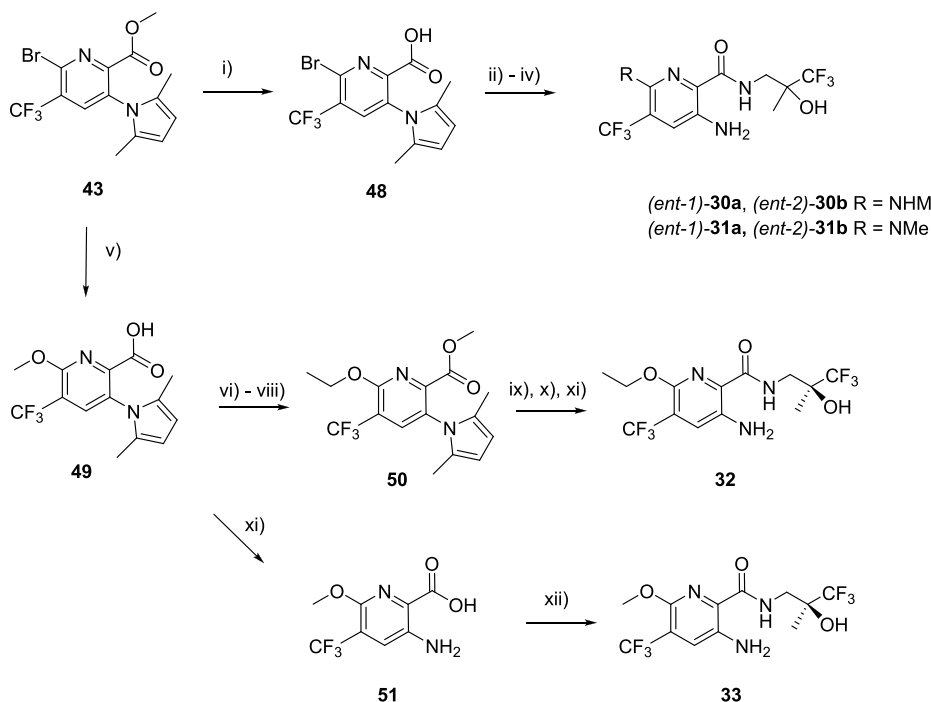
^aReagents and conditions: (i) MeB(OH)₂, Pd(dppf)Cl₂, K₃PO₄, toluene–water, μ W 150°C, 43%; (ii) 41, HATU, Et₃N, CH₂Cl₂, RT, 70%; (iii) 2,5-hexanedione, TsOH, toluene, reflux, 73%; (iv) EtB(OH)₂, Pd(dppf)Cl₂, Cs₂CO₃, THF–water, μ W 150°C, 22%; (v) NaOH, aq THF, RT, 54%; (vi) 41, HATU, Et₃N, NMP, RT, 19%; (vii) NH₂OH·HCl, Et₃N, EtOH–water, reflux, 21% then chiral HPLC; (viii) TMS-CF₃, KF, CuI, DMF–NMP μ W, 100°C, 33%; (ix) NH₂OH·HCl, Et₃N, EtOH–water, reflux, 73%; (x) (S)-41, HATU, DIPEA, DMF, RT, 75%.

oxazinedione intermediate, from which amides 15 and 16 were prepared by ring opening with the appropriate amine (Scheme 1).

The picolinamide analogue 13 was synthesized from commercially available 3-nitro-5-(trifluoromethyl)pyridin-2-one according to Scheme 2. Chlorination of the pyridone with phosphorus oxychloride followed by copper mediated displacement of the chlorine with cyanide and tin chloride reduction of the nitro group afforded the 2-cyanopyridine 36, which was readily hydrolyzed with concentrated hydrochloric acid to the 3-amino picolinic acid 37. Esterification followed by selective bromination at the 6-position of the pyridine ring allowed installation of the furan group by palladium catalyzed Stille cross coupling. The 6-bromo-3-amino picolinamide derivatives 17–25 were synthesized from the bromo amino picolinic ester 39 by HATU coupling from intermediate chemistry also described in Scheme 2. The same amide coupling conditions afforded 26 in 51% yield from 37. The racemic amino alcohol 41 was synthesized by a Henry reaction between nitromethane and methyltrifluoromethyl ketone shown in Scheme 3. Hydro-

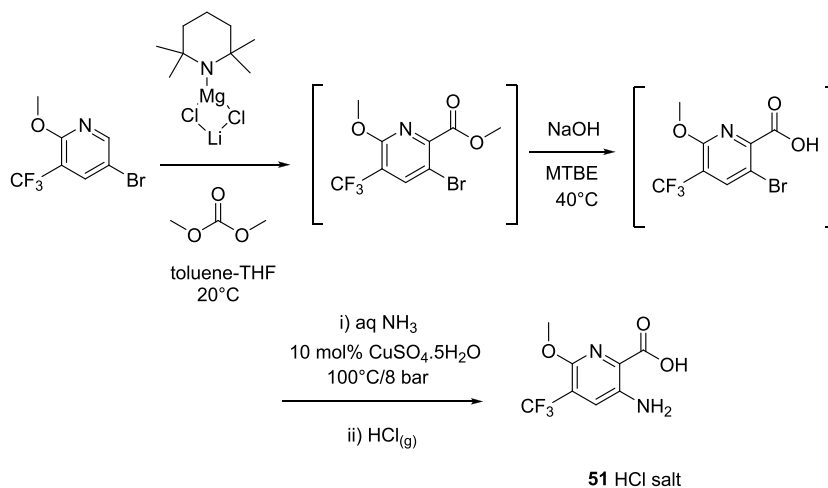
genation of the nitro group in 40 over palladium on charcoal afforded the desired amine in sufficient purity for the subsequent HATU coupling reactions. The (S)-enantiomer of 41 was obtained in 97.4% ee via resolution of the (+)-tartrate salt, with the absolute configuration confirmed by X-ray crystallography of the free base (Supporting Information Figure S2).

For further substitution at the picolinamide 6-position to initially access the 6-methyl analogue 27, one pot Suzuki coupling and ester hydrolysis delivered intermediate 42, which was readily coupled under HATU conditions (Scheme 4). Protection of the amino group as the 2,5-dimethylpyrrole afforded the versatile intermediate 43, which allowed access to 6-ethyl analogue 28 via Suzuki coupling as well as the 6-trifluoromethyl analogue 29 through treatment with Ruppert's reagent in moderate yield (Scheme 4). Intermediate 43 also served as a precursor to the 6-amino analogues 30 and 31 via nucleophilic displacement of bromine (Scheme 5). Ester hydrolysis of 43 in the presence of methanolic NaOH led to concomitant replacement of bromine by methoxy to afford intermediate 49, which was transformed to the 6-ethoxy

Scheme 5. Synthesis of Compounds 30–33^a

^aReagents and conditions: (i) aq NaOH, THF, RT, 97%; (ii) aq Me₂NH or MeNH₂, THF, RT, 56–92%; (iii) **41**, HATU, Et₃N, NMP, RT, 52–78%; (iv) NH₂OH·HCl, Et₃N, EtOH–water, reflux, then chiral HPLC, 34–36%; (v) aq NaOH, MeOH, 60°C, 97%; (vi) cat H₂SO₄, MeOH, reflux, 75%; (vii) TMSCl, KI, MeCN, reflux, 54%; (viii) EtOH, DEAD, Ph₃P, dioxane, RT, 61%; (ix) aq NaOH, THF, reflux, 26%; (x) (S)-**41**, HATU, DIPEA, DMF, RT, 89%; (xi) NH₂OH·HCl, Et₃N, EtOH–water, reflux, 37–53%; (xii) (S)-**41**, HATU, DIPEA, NMP, RT, 59%.

Scheme 6. Process Chemistry Route to Key Intermediate 51



intermediate **50** through a sequence of esterification, demethylation, and Mitsunobu reaction with ethanol, leading to compound **32**. Finally, compound **33** could be accessed directly from picolinic acid intermediate **51**. Subsequent to this discovery phase synthesis, alternative scaled up preparations of **33** have been reported,⁴⁹ including the truncated process chemistry route shown in Scheme 6, which delivered the key intermediate **51** in 72% yield from 5-bromo-2-methoxy-3-(trifluoromethyl)pyridine.

CONCLUSION AND PERSPECTIVE

High throughput screening identified the anthranilate hit **6** as novel potentiator of delF508 and WT CFTR channels. In the

absence of any available *in vivo* PK–PD or disease models for CF, an optimization strategy focused on improving LLE and maximizing free drug exposure was employed. With this approach, the scaffold was evolved to the advanced candidates **22** and **33**, which both showed potent potentiation of CFTR in primary HBECs from either CF or non-CF patient donors, comparable to the reference potentiator ivacaftor **1**. The potential for reactivity of the 6-bromopyridine moiety in **22** presented a concern, with human and rat *in vitro* and rat *in vivo* metabolite identification experiments providing contrasting results on GSH adduct formation. To further derisk compound progression, an exploratory 14-day rat toxicology study was conducted, which clearly indicated a superior profile for **33**

compared to 22. Based on this differentiation, 33 was advanced into the clinic and shown to be safe and well-tolerated in healthy volunteers. An initial clinical PoC as evidenced by improvement in lung function was obtained in CF patients with Class III and IV CFTR mutations. This was followed by a second clinical study in COPD patients with chronic bronchitis, which showed significant improvement in lung function as well as evidence of reduction in a qualified systemic COPD inflammatory biomarker. Compound 33, now known as icentricaftor, is in ongoing clinical development for COPD with chronic bronchitis.

■ EXPERIMENTAL SECTION

CFTR Membrane Potential Assay. Chinese hamster ovary (CHO) cells stably expressing the delF508-CFTR channel were maintained at 37 °C in 5% v/v CO₂ at 100% humidity in Modified Eagles medium (MEM) supplemented with 8% v/v fetal calf serum, 100 μg/mL methotrexate, and 100 U/mL penicillin/streptomycin. Cells were grown in 225 cm² tissue culture flasks. For membrane potential assays, cells were seeded into 96-well plates at 40 000 cells per well, allowed to adhere, and then maintained at 26 °C for 48 h to facilitate channel insertion. The membrane potential screening assay utilized a low chloride ion containing extracellular solution (~5 mM) combined with a double addition protocol. The first addition was of buffer with or without test compounds followed 5 min later by an addition of forskolin (1–20 μM); this protocol favors maximum chloride efflux in response to delF508-CFTR activation. The delF508-CFTR mediated chloride ion efflux led to a membrane depolarization which was optically monitored by FLIPR, and efficacy of compounds was compared to a known potentiator such as PG-01. Low chloride ion extracellular solution was prepared as follows: 120 mM Na-glucuronate, 1.2 mM CaCl₂, 3.3 mM KH₂PO₄, 0.8 mM K₂HPO₄, 1.2 mM MgCl₂, 10.0 mM D-glucose, 20.0 mM HEPES, pH 7.4 with NaOH. The FLIPR dye (Molecular Devices) was made up pursuant to the manufacturer's instructions in extracellular solution at 10× final concentration and stored as 1 mL aliquots at –20 °C. Concentration–response curves were fitted using nonlinear regression fit, sigmoidal dose response with variable slope using GraphPad Prism.

CFTR Ion Works Quattro Assay. CHO cells stably expressing the delF508-CFTR channel were maintained at 37 °C in 5% v/v CO₂ at 100% humidity in D-MEM supplemented with 10% (v/v) FCS, 100 U/mL penicillin/streptomycin, 1% (v/v) NEAA, 1 mg/mL Zeocin, and 500 μg/mL Hygromycin B. For experiments, cells were grown in 225 cm² tissue culture flasks until near confluence and then cultured at 26 °C for 48–72 h to facilitate channel insertion. Cells were removed from the flask and resuspended in either extracellular recording solution for immediate experimentation or alternatively in growth medium supplemented with 10% v/v DMSO and frozen to –80 °C as 1–2 mL aliquots for use at a later date. Cells, at a density of 1.5–3 million per mL, were placed on the Quattro system and added to the planar patch array, and seals were allowed to establish for 5–10 min. After assessing seal resistances (commonly >50 MΩ), whole-cell access was obtained by perforation with 100 μg/mL amphotericin B. Baseline currents were measured by a precompound scan obtained by application of a voltage ramp from –100 to +100 mV. This was followed by addition of either buffer or test compound diluted in the extracellular solution supplemented with 20 μM forskolin to each of the 384 wells of the planar patch array. After the incubation step (5–20 min), the postcompound currents were measured again by application of a voltage ramp from –100 to +100 mV. The difference in currents between the pre- and postcompound scans defined the efficacy of CFTR potentiation. The efficacies of compounds were compared to a known potentiator such as PG-01. Concentration–response curves were fitted using nonlinear regression fit, sigmoidal dose response with variable slope using GraphPad Prism.

CFTR Ion Transport Assays with FRT Cells. FRT cells stably expressing delF508-CFTR, G551D-CFTR, or WT-CFTR were cultured on plastic in Coon's modified F-12 medium supplemented

with 32 mM NaHCO₃, 10% v/v fetal bovine serum, 2 mM L-glutamine, 100 U/mL penicillin, 100 μg/mL streptomycin, and 30 μg/mL hygromycin B as the growth medium. For Ussing chamber experiments, the cells were grown as polarized epithelia on Snapwell permeable support inserts (500 000 cells/insert in growth medium) and cultured for 7 to 9 days. The inserts were fed with fresh Coon's modified F-12 growth medium every 48 h and 24 h prior to Ussing chamber experiments. To increase the delF508 CFTR protein expression at the cell surface, plates were incubated at 27 °C for 48 h before performing an Ussing chamber experiment. The FRT epithelial cells were used as monolayer cultures on permeable supports. Cl[–] current was measured using the short circuit current technique (*I*_{sc}) under an imposed basolateral to apical Cl[–] gradient in Ussing chambers. Ussing chamber studies were likewise conducted at 27 °C, whereas for WT CFTR and G551D CFTR cells, all protocols were conducted at 37 °C. Under these conditions, the effects of cumulative additions of test compounds on delF508 CFTR, G551D, or WT CFTR currents could be quantitated with both potency and efficacy end points. Compounds were added to both the apical and basolateral sides subsequent to addition of forskolin at concentrations corresponding to the EC₂₀ value for WT CFTR (370 nM) and the EC₅₀ values for F508del and G551D CFTR (both 20 μM). Efficacy of compounds was compared to a known potentiator such as PG-01 or ivacaftor, and concentration–response curves were fitted using nonlinear regression fit, sigmoidal dose response with variable slope using GraphPad Prism.

CFTR Ion Transport Assays with Primary HBEC. HBEC were expanded and cryopreserved as previously described.⁵⁰ On thawing, cells were further expanded using the same method as described above. When at 90% confluency, cells were seeded onto collagen coated polyester 12 mm inserts in differentiation media containing 50% DMEM in BEGM with the same supplements as above but without triiodothyronine and a final retinoic acid concentration of 50 nM. Cells were maintained submerged for the first 7 days in culture. After 7 days submerged, the cells were exposed to air liquid interface (ALI) for the remainder of the culture period. Cells were used between days 14 and 28 after establishment of the ALI. At all stages of culture, cells were maintained at 37 °C in 5% CO₂. Collagen coated snapwell inserts (prepared as described in the [Supporting Information](#)) were mounted in vertical diffusion chambers bathed with continuously gassed physiological salt solution (5% CO₂ in O₂; pH 7.4) maintained at 37 °C. Cells were voltage clamped to 0 mV, and transepithelial resistance (RT) was measured by applying a 1 mV pulse at 30-s intervals and calculating RT by Ohm's law. Changes in *I*_{sc} in response to amiloride, forskolin, CFTR potentiators, and blockers were recorded. Compound additions were made by removal of 0.5 mL of bathing solution and replacement of the solution containing the test compound to produce the stated final bath concentration. Amiloride was added apically (10 μM) at the start of all studies to determine the amiloride-sensitive *I*_{sc}. Following amiloride addition, forskolin at a concentration corresponding to the EC₂₀ for WT CFTR (100 nM) or the EC₅₀ for F508del CFTR (20 μM) was added to both the apical and basolateral chambers, followed by cumulative concentrations of test compounds. At the end of the experiment, CFTRinh172 (30 μM apical) was added to inhibit all CFTR mediated anion transport. Efficacy of compounds was compared to the known potentiator ivacaftor, and concentration–response curves were fitted using nonlinear regression fit, sigmoidal dose response with variable slope using GraphPad Prism.

Pharmacokinetic Studies and *In Vitro* Profiling Assays. All animal experiments reported were conducted in compliance with local institutional guidelines at NIBR Basel, East Hanover and Horsham. *In vivo* PK study details, plasma protein binding assays, and safety profiling panel targets are described in the [Supporting Information](#) available online. Microsomal clearance and PAMPA permeability assays have been reported previously.⁵¹

Chemistry. The purity of all final compounds was ≥95%. ¹H NMR spectra were measured at 400 MHz; ¹³C NMR spectra were measured 100 MHz, and ¹⁹F NMR spectra were measured 376 MHz on a Bruker AV400 NMR spectrometer. Low resolution mass spectra (LRMS) were determined by LCMS recorded on an Agilent 1100 LC system with a Waters Xterra MS C18 4.6 × 100 5 μM column, eluting with 5–95% 10

mM aqueous ammonium bicarbonate in acetonitrile over 2.5 min with negative ion electrospray ionization or 5–95% water +0.1% TFA in acetonitrile with positive ion electrospray ionization. $[\text{MH}]^+$ refers to monoisotopic molecular mass. Gas chromatographs (GC) were recorded on an Agilent 7890A instrument with a gradient of 25 °C/min from 40 to 220 °C then 40 °C/min to 280 °C. Flash chromatography was conducted with prepacked silica columns using a Teledyne ISCO CombiFlash system. Microwave reactions were conducted in a Biotage Emrys Personal Chemistry Optimizer Microwave Synthesizer. Microanalysis for carbon, hydrogen, and nitrogen was carried out on a LECO CHNS-932 analyzer using ethylenediaminetetraacetic acid as the primary calibration standard.

Methyl 2-Amino-5-(furan-2-yl)-4-(trifluoromethyl)benzoate (6). A solution of 2-amino-4-(trifluoromethyl)benzoic acid (3 g, 14.62 mmol) and concentrated H_2SO_4 (3.9 mL, 73.1 mmol) in MeOH (50 mL) was heated at reflux overnight. Additional concentrated H_2SO_4 (3.9 mL, 73.1 mmol) was added, and reflux continued for a further 48 h. The MeOH was evaporated; the residue was added to a stirred solution of saturated NaHCO_3 sufficient to neutralize residual acid, and the resulting solution was extracted into EtOAc. The organic phase was washed with saturated brine and dried (MgSO_4) and the solvent was evaporated to afford methyl 2-amino-4-(trifluoromethyl)benzoate 7 as pale yellow crystals (2.54 g, 75%). LRMS $\text{C}_9\text{H}_8\text{F}_3\text{NO}_2$ requires M^+ 219.05, found $[\text{MH}]^+$ 220.1. ^1H NMR ($\text{DMSO}-d_6$) 3.82 (3H s), 6.78 (1H dd $J = 8.4, 1.6$), 7.80 (2H br s), 7.14 (1H d $J = 0.9$), 7.88 (1H d $J = 8.3$).

Ag_2SO_4 (2.134 g, 6.84 mmol) was added to a solution of methyl 2-amino-4-(trifluoromethyl)benzoate 7 (1.5 g, 6.84 mmol) followed by iodine (1.737 g, 6.84 mmol). The mixture was stirred at RT for 3 h and filtered, and the filtrate was evaporated onto silica gel prior to purification by flash chromatography eluting with 3:1 isohexanes-EtOAc to afford methyl 2-amino-5-iodo-4-(trifluoromethyl)benzoate 9 as an orange solid (0.435 g, 18%). LRMS $\text{C}_9\text{H}_7\text{F}_3\text{INO}_2$ requires M^+ 344.95, found M^+ 345.0. ^1H NMR ($\text{DMSO}-d_6$) 3.85 (3H s), 7.08 (2H br s), 7.30 (1H s), 8.23 (1H s).

$\text{Pd}(\text{Ph}_3\text{P})_4$ (17 mg, 0.01 mmol) was added to a degassed solution of tri-*n*-butyl-2-furylstannane (0.136 mL, 0.48 mmol) and methyl 2-amino-5-iodo-4-(trifluoromethyl)benzoate 9 (0.1 g, 0.28 mmol) in dioxane (3 mL). The reaction was heated at reflux for 5 h and then filtered and evaporated onto silica gel. Purification by flash chromatography eluting with 5:1 isohexanes-EtOAc followed by isohexane trituration afforded methyl 2-amino-5-(furan-2-yl)-4-(trifluoromethyl)benzoate 6 as a beige solid (51 mg, 62%). LRMS $\text{C}_{13}\text{H}_{10}\text{F}_3\text{NO}_3$ requires M^+ 285.06, found $[\text{MH}]^+$ 286.2. ^1H NMR (CDCl_3) 3.94 (3H s), 6.02 (2H br s), 6.48 (1H dd $J = 3.4, 1.9$), 6.53 (1H d $J = 3.4$), 7.06 (1H s), 7.51 (1H d $J = 1.7$), 8.21 (1H s).

Methyl 2-Amino-5-(oxazol-2-yl)-4-(trifluoromethyl)benzoate (10). $\text{Pd}(\text{Ph}_3\text{P})_4$ (17 mg, 0.01 mmol) was added to a degassed solution of tri-*n*-butyl-2-oxazolylstannane (0.091 mL, 0.44 mmol) and methyl 2-amino-5-iodo-4-(trifluoromethyl)benzoate 9 (0.1 g, 0.28 mmol) in dioxane (4 mL). The reaction was heated at reflux for 5 h and then filtered and evaporated onto silica gel. Purification by flash chromatography eluting with 9:1 isohexanes-EtOAc followed by isohexane trituration afforded methyl 2-amino-5-(oxazol-2-yl)-4-(trifluoromethyl)benzoate 10 (28 mg, 34%) as a pale yellow solid. LRMS $\text{C}_{12}\text{H}_9\text{F}_3\text{N}_2\text{O}_3$ requires M^+ 286.06, found $[\text{MH}]^+$ 287.0. ^1H NMR ($\text{DMSO}-d_6$) 3.86 (3H s), 7.40 (1H br s), 7.43 (2H overlapping d $J = 8$), 8.18 (1H s), 8.34 (1H s).

Methyl 2-Amino-5-(pyridin-3-yl)-4-(trifluoromethyl)benzoate (11). Methyl 2-amino-5-iodo-4-(trifluoromethyl)benzoate 9 (0.100 g, 0.290 mmol) followed by $\text{Pd}(\text{dppf})_2\text{Cl}_2$ (24 mg, 0.029 mmol) were added to a solution of 3-pyridineboronic acid (53 mg, 0.435 mmol) and Na_2CO_3 (0.154 g, 1.449 mmol) in DME (5 mL) in a microwave vial. Additional DME (5 mL) was added, and then the vial was capped and irradiated at 100 °C for 1 h. The reaction mixture was evaporated onto silica gel and purified by flash chromatography eluting with 3:1 isohexanes-EtOAc to afford methyl 2-amino-5-(pyridin-3-yl)-4-(trifluoromethyl)benzoate 11 as a white solid (64 mg, 75%). LRMS $\text{C}_{14}\text{H}_{11}\text{F}_3\text{N}_2\text{O}_2$ requires M^+ 296.08, found $[\text{MH}]^+$ 297.1. ^1H NMR ($\text{DMSO}-d_6$) 3.81 (3H s), 7.11 (2H br s), 7.34 (1H s), 7.45 (1H dd $J =$

7.8, 4.8), 7.65 (1H s), 7.71 (1H d $J = 7.8$), 8.47 (1H s), 8.59 (1H dd $J = 4.8, 1.3$).

(±)-Methyl 2-Amino-5-(tetrahydrofuran-2-yl)-4-(trifluoromethyl)benzoate (12). A solution of methyl 2-amino-5-(furan-2-yl)-4-(trifluoromethyl)benzoate 6 (0.100 g, 0.351 mmol) in EtOH (10 mL) was hydrogenated over Raney Nickel (70 °C/70 psi) for 15 h using an H-Cube flow reactor. The reaction mixture was evaporated onto silica gel and purified by flash chromatography eluting with 100% isohexanes-40% isohexanes/60% EtOAc gradient to afford methyl 2-amino-5-(tetrahydrofuran-2-yl)-4-(trifluoromethyl)benzoate 12 as a white solid (25 mg, 25%). LRMS $\text{C}_{13}\text{H}_{14}\text{F}_3\text{NO}_3$ requires M^+ 289.09, found $[\text{MH}]^+$ 290.2. ^1H NMR ($\text{DMSO}-d_6$) 1.45 (1H m), 1.88 (2H m), 2.16 (1H m), 3.71 (1H dd $J = 14.9, 7.5$), 3.78 (3H s), 4.00 (1H dd $J = 14.4, 7.0$), 4.79 (1H t $J = 6.7$), 6.86 (2H br s), 7.10 (1H s), 7.93 (1H s).

Methyl 3-Amino-6-(furan-2-yl)-5-(trifluoromethyl)picolinate (13). DMF (1.414 mL, 18.26 mmol) was added dropwise to POCl_3 (25.5 mL, 274 mmol) at RT, followed by 3-nitro-5-(trifluoromethyl)pyridin-2-ol (9.5 g, 45.7 mmol) portionwise, and the reaction mixture was heated at 110 °C for 45 min. The reaction was cooled to RT and quenched by addition to water with vigorous stirring. The resultant suspension was extracted with EtOAc and the organic phase was dried (MgSO_4) and evaporated to afford 2-chloro-3-nitro-5-(trifluoromethyl)pyridine 34 as a pale yellow oil (8.79 g, 83%). ^1H NMR ($\text{DMSO}-d_6$) 9.16 (1H s), 9.30 (1H s).

CuCN (3.56 g, 39.7 mmol) was added to a solution of 2-chloro-3-nitro-5-(trifluoromethyl)pyridine 34 (9.0 g, 39.7 mmol) in NMP (17 mL) and was heated to 175 °C for 40 min. After cooling to RT, the reaction mixture was partitioned between water/EtOAc and the biphasic mixture was filtered through Celite and washed with EtOAc. The organic phase was dried (MgSO_4), evaporated and purified by flash chromatography (3:1 isohexanes-EtOAc elution). Recrystallization from 3:1 isohexanes-EtOAc afforded 3-nitro-5-(trifluoromethyl)picolinonitrile 35 (3.65 g, 42%) as a white crystalline solid. ^1H NMR ($\text{DMSO}-d_6$) 9.32 (1H s), 9.64 (1H s).

SnCl_2 (14.41 g, 76 mmol) was added to a solution of 3-nitro-5-(trifluoromethyl)picolinonitrile 35 (3.3 g, 15.20 mmol) in EtOH (30 mL), and the reaction was heated at reflux for 3 h. The solvent was evaporated, and the residue was taken up in EtOAc and then washed with saturated NaHCO_3 . The washings were diluted with water and back extracted with EtOAc and the combined organic phases were dried (MgSO_4) then evaporated to afford crude 3-amino-5-(trifluoromethyl)picolinonitrile 36 (2.57 g, 45%) as a yellow solid, which was taken into conc HCl (13.4 mL, 134 mmol) and heated to reflux for 4 h. The solvent was evaporated to afford 3-amino-5-(trifluoromethyl)picolinic acid hydrochloride 37 (3.02 g, 89%) as a yellow solid. ^1H NMR ($\text{DMSO}-d_6$) 7.21 (1H s), 7.35 (1H s), 7.47 (1H s), 7.70 (1H s), 8.21 (1H s).

Thionyl chloride (1.083 mL, 14.84 mmol) was added to a solution of 3-amino-5-(trifluoromethyl)picolinic acid hydrochloride 37 (3.0 g, 12.37 mmol) in MeOH (25 mL), and the reaction mixture heated to reflux. Two further portions of thionyl chloride (1.083 mL, 14.84 mmol) were added after 16 and 24 h, and after a total of 56 h, the solvent was evaporated. The residue was partitioned between saturated NaHCO_3 and EtOAc, then the organic phase was dried (MgSO_4) and evaporated. Purification via flash chromatography (3:1 isohexanes-EtOAc elution) afforded methyl 3-amino-5-(trifluoromethyl)picolinate 38 (1.75 g, 64%) as a yellow solid. ^1H NMR ($\text{DMSO}-d_6$) 3.85 (3H s), 7.01 (2H br s), 7.6 (1H d $J = 1.3$), 8.13 (1H d $J = 1.4$).

A suspension of methyl 3-amino-5-(trifluoromethyl)picolinate 38 (1.0 g, 4.54 mmol) and conc H_2SO_4 (0.484 mL, 9.08 mmol) in water was briefly heated to 100 °C (heat gun) to aid dissolution and then cooled to RT. A solution of bromine (0.234 mL, 4.54 mmol) in acetic acid (3.12 mL, 54.5 mmol) was added dropwise, and the resultant suspension was stirred for 2 h. The solid was collected by filtration, washed with water, dried and recrystallized from hot MeOH to afford methyl 3-amino-6-bromo-5-(trifluoromethyl)picolinate 39 (0.905 g, 68%) as yellow needles. ^1H NMR ($\text{DMSO}-d_6$) 3.86 (3H s), 7.15 (1H br s), 7.77 (1H s).

Pd(Ph₃P)₄ (39 mg, 0.033 mmol) was added to a solution of methyl 3-amino-6-bromo-5-(trifluoromethyl)picolinate **39** (0.100 g, 0.334 mmol) and tri-*n*-butyl-2-furylstannane (0.105 mL, 0.334 mmol) in dioxane (5 mL), and the reaction was heated at reflux for 5 h. The reaction was evaporated onto silica gel, and purification by flash chromatography eluting with 4:1 isohexanes-EtOAc followed by hot isohexane trituration afforded methyl 3-amino-6-(furan-2-yl)-5-(trifluoromethyl)picolinate **13** (55 mg, 57%) as a pale yellow solid. LRMS C₁₂H₉F₃N₂O₃ requires M⁺ 286.06, found [MH]⁺ 287.1. ¹H NMR (DMSO-*d*₆) 3.87 (3H s), 6.61 (1H dd *J* = 3.2, 1.7), 6.76 (1H d *J* = 3.2), 7.75 (1H s), 7.80 (1H s).

2-Amino-5-(furan-2-yl)-4-(trifluoromethyl)benzoic acid (14). A solution of methyl 2-amino-5-(furan-2-yl)-4-(trifluoromethyl)benzoate **6** (2.28 g, 7.99 mmol) and 4 M NaOH (4 mL, 15.98 mmol) in EtOH (25 mL) was stirred at RT for 16 h. The solvent was evaporated, and the residue was diluted with water and then neutralized with 0.1 M HCl. The resultant precipitate was collected by filtration and dried to afford 2-amino-5-(furan-2-yl)-4-(trifluoromethyl)benzoic acid **14** (1.99 g, 84%) as a yellow solid. LRMS C₁₁H₇F₃N₂O₃ requires M⁺ 271.05, found [MH]⁺ 272.2. ¹H NMR (CDCl₃) 6.02 (2H br s), 6.49 (1H dd, *J* = 3.4, 1.9), 6.55 (1H d *J* = 3.4), 7.08 (1H s), 7.51 (1H d *J* = 1.8), 8.28 (1H s), 12.00–9.41 (1H br s).

2-Amino-5-(furan-2-yl)-*N*-methyl-4-(trifluoromethyl)benzamide (15). A solution of triphosgene (43 mg, 0.147 mmol) in DCM (1 mL) was added to a solution of 2-amino-5-(furan-2-yl)-4-(trifluoromethyl)benzoic acid **14** (0.100 g, 0.368 mmol) and pyridine (59 μL, 0.736 mmol) in MeCN (2 mL). The reaction was heated to reflux for 30 min and cooled to RT, and the resultant solid was collected by filtration, taken into DCM, and washed with water. The organic phase was dried (MgSO₄) and evaporated to afford 6-(furan-2-yl)-7-(trifluoromethyl)-2*H*-benzo[d][1,3]oxazine-2,4(1*H*)-dione (89 mg, 81%) as a light brown solid. ¹H NMR (DMSO-*d*₆) 6.67 (1H dd *J* = 3.4, 1.8), 6.88 (1H d *J* = 3.4), 7.56 (1H s), 7.89 (1H d *J* = 1.2), 8.18 (1H s), 12.07 (1H s).

Methylamine (40% aq; 26 μL, 0.336 mmol) was added to a solution of 6-(furan-2-yl)-7-(trifluoromethyl)-2*H*-benzo[d][1,3]oxazine-2,4(1*H*)-dione (50 mg, 0.168 mmol) in THF (2 mL). The reaction was stirred at RT for 1.5 h, and then additional methylamine (40% aq; 52 μL, 0.672 mmol) was added. After a further 20 min, the reaction mixture was evaporated onto silica gel and purified by flash chromatography (3:1 isohexanes-EtOAc elution) to afford 2-amino-5-(furan-2-yl)-*N*-methyl-4-(trifluoromethyl)benzamide **15** (21 mg, 44%) as a white solid. LRMS C₁₃H₁₁F₃N₂O₂ requires M⁺ 284.08, found [MH]⁺ 285.2. ¹H NMR (DMSO-*d*₆) 2.75 (3H d *J* = 4.5), 6.56 (2H s), 6.93 (2H s), 7.19 (1H s), 7.73 (1H s), 7.77 (1H s), 8.51 (1H br s).

2-Amino-5-(furan-2-yl)-*N,N*-dimethyl-4-(trifluoromethyl)benzamide (16). A solution of 2-amino-5-(furan-2-yl)-4-(trifluoromethyl)benzoic acid **14** (27 mg, 0.1 mmol) and triphosgene (10 mg, 0.34 mmol) in THF (1 mL) was shaken for 1 h, and the solvent was evaporated. The residue was triturated with Et₂O and taken into DMF (1 mL). Dimethylamine (13 μL, 0.2 mmol) was added, and the reaction was shaken for 16 h. The crude product was purified by elution through a solid phase extraction cartridge (PE-AX SCX2) to afford 2-amino-5-(furan-2-yl)-*N,N*-dimethyl-4-(trifluoromethyl)benzamide **16** (4 mg, 13%) as a white solid. LRMS C₁₄H₁₃F₃N₂O₂ requires M⁺ 298.09, found [MH]⁺ 299.0. ¹H NMR (CDCl₃) 3.1 (6H s), 4.63 (2H br s), 6.48 (1H dd *J* = 3.4, 1.8), 6.54 (1H d *J* = 3.3), 7.08 (1H s), 7.28 (1H s), 7.49 (1H d *J* = 1.6).

3-Amino-6-bromo-*N*-methyl-5-(trifluoromethyl)picolinamide (17). Four molar aq NaOH (14.04 mL, 28 mmol) was added to a suspension of methyl 3-amino-5-(trifluoromethyl)picolinate **38** (1.4 g, 4.68 mmol) in MeOH (15 mL) and the reaction was stirred at RT for 16 h. The solvent was evaporated, the residue was taken into water, acidified with 5 M HCl, and extracted twice with EtOAc. The combined organic phases were washed with water and brine and then dried (MgSO₄). Evaporation and trituration with Et₂O afforded 3-amino-6-bromo-5-(trifluoromethyl)picolinic acid (1.25 g, 94%) as a yellow solid. ¹H NMR (DMSO-*d*₆) 7.17 (2H br s), 7.74 (1H s) 13.24 (1H br s).

N-Methylmorpholine (0.104 mL, 1.053 mmol) was added to a solution of 3-amino-6-bromo-5-(trifluoromethyl)picolinic acid (0.150 g, 0.526 mmol) and HATU (0.200 g, 0.526 mmol) in DMF (2.5 mL). The mixture was stirred at RT for 5 min prior to addition of methylamine (2 M THF, 0.526 mL, 1.053 mmol). After standing at RT for 48 h, the reaction was poured into water and extracted twice with EtOAc. The combined organic extracts were dried (MgSO₄) and evaporated. Purification by flash chromatography (0–100% EtOAc-isohexanes gradient elution) afforded 3-amino-6-bromo-*N*-methyl-5-(trifluoromethyl)picolinamide **17** (0.103 g, 66%) as a white solid. LRMS C₈H₅BrF₃N₃O requires M⁺ 296.97, found [MH]⁺ 298.0. ¹H NMR (DMSO-*d*₆) 2.78 (3H d *J* = 4.7), 7.26 (2H br s), 7.67 (1H s), 8.47 (1H br d *J* = 4.7).

3-Amino-6-bromo-5-(trifluoromethyl)-*N*-(3,3,3-trifluoropropyl)picolinamide (18). Prepared with the same procedure used for **17**, using 3,3,3-trifluoropropylamine and isolated as a yellow oil (0.119 g, 89%). LRMS C₁₀H₈BrF₆N₃O requires M⁺ 378.98, found [MH]⁺ 380.1. ¹H NMR (DMSO-*d*₆) 2.56 (2H m), 3.51 (2H q *J* = 6.8), 7.28 (2H br s), 7.70 (1H s), 8.69 (1H t *J* = 6.0).

(±)-3-Amino-6-bromo-*N*-(2-hydroxypropyl)-5-(trifluoromethyl)picolinamide (19). Prepared with the same procedure used for **17**, using (±)-1-amino-2-propanol and isolated as an off-white solid (0.140 g, 80%). LRMS C₁₀H₁₁BrF₃N₃O₂ requires M⁺ 341.00, found [MH]⁺ 342.0. ¹H NMR (DMSO-*d*₆) 1.05 (3H d *J* = 6.3), 3.14 (1H m), 3.14 (1H m), 3.29 (1H m), 3.78 (1H m), 4.84 (1H d *J* = 4.8), 7.28 (2H br s), 7.69 (1H s), 8.30 (1H t *J* = 5.9).

(*S*)-3-Amino-6-bromo-*N*-(3,3,3-trifluoro-2-hydroxypropyl)-5-(trifluoromethyl)picolinamide (20). Prepared with the same procedure used for **17**, starting from (*S*)-3-amino-1,1,1-trifluoro-2-propanol (50 mg, 36%). LRMS C₁₀H₈BrF₆N₃O₂M⁺ requires 394.97, found [MH]⁺ 396.0. ¹H NMR (DMSO-*d*₆) 3.40 (1H m), 3.58 (1H m), 4.24 (1H m), 6.50 (1H br s), 7.29 (2H br s), 7.71 (1H s), 8.56 (1H br s).

(*R*)-3-Amino-6-bromo-*N*-(3,3,3-trifluoro-2-hydroxypropyl)-5-(trifluoromethyl)picolinamide (21). Prepared with the same procedure used for **17**, starting from (±)-3-amino-1,1,1-trifluoro-2-propanol, with separation of the enantiomers via preparative chiral SFC (Chiralpak AD-H column, 12% [2-propanol + 0.1% DEA]/88% CO₂ elution), (85 mg, 15%) retention time 3.1 min, >98% ee (vs retention time 2.2 min for **20**). LRMS C₁₀H₈BrF₆N₃O₂M⁺ requires 394.97, found [MH]⁺ 396.0. ¹H NMR (DMSO-*d*₆) 3.40 (1H m), 3.58 (1H m), 4.24 (1H m), 6.50 (1H br s), 7.29 (2H br s), 7.71 (1H s), 8.56 (1H br s).

(*S*)-3-Amino-6-bromo-*N*-(3,3,3-trifluoro-2-hydroxy-2-methylpropyl)-5-(trifluoromethyl)picolinamide (22) and (*R*)-3-Amino-6-bromo-*N*-(3,3,3-trifluoro-2-hydroxy-2-methylpropyl)-5-(trifluoromethyl)picolinamide (23). LiOH (11.7 g, 0.279 mol) was dissolved in distilled water (1 L), and the solution was cooled to 10 °C. Nitromethane (170 g, 128 mL, 27.9 mol) was added followed by cetyltrimethylammonium chloride (120 g, 0.377 mol) and magnesium sulfate (77 g, 0.558 mol). The cloudy suspension was maintained at 5 °C in an ice bath while trifluoroacetone (500 g, 400 mL, 4.462 mol) was added dropwise. The internal temperature rose to 15 °C and upon cooling, the reaction mixture was stirred at 0 °C for 3 h. The reaction mixture was diluted with TBME (1 L) and the phases separated. The organic phase was extracted with brine (2 × 500 mL) and the aqueous phase was washed with TBME (500 mL). To the combined organic phases was added Biotage supercation exchange resin (500 g, to remove the cetyltrimethylammonium chloride) and the mixture was stirred at RT over the weekend. The suspension was filtered and washed with TBME (2 L). The mother liquor was concentrated to give the product as a yellow liquid (625 g). NMR showed remaining cetyltrimethylammonium chloride, so the product was dissolved in TBME (1 L) and scavenged again with Biotage supercation exchange resin (500 g) overnight at RT. The suspension was filtered and washed with TBME (2 L). The mother liquor was concentrated to afford 1,1,1-trifluoro-2-methyl-3-nitropropan-2-ol **40** (457 g, 95%) as a pale yellow oil. ¹H NMR (CDCl₃) 1.57 (3H s), 4.56 (1H d *J* = 12.5), 4.73 (1H d *J* = 12.5).

A suspension of 10% Pd/C (2.4 g) and 1,1,1-trifluoro-2-methyl-3-nitropropan-2-ol **40** (24.29 g, 140 mmol) in EtOH (250 mL) was

hydrogenated at 5 bar pressure for 2 h at RT. The reaction mixture was filtered through Celite, evaporated and taken into MeOH (50 mL). HCl (1.25 M EtOH solution; 112 mL, 140 mmol) was added. The solution was stirred at RT for 1 h and evaporated to afford (±)-3-amino-1,1,1-trifluoro-2-methylpropan-2-ol **41** hydrochloride (22.72 g, 72%) as a white solid. ¹H NMR (DMSO-*d*₆) 1.40 (3H s), 2.99 (2H s), 6.84 (1H br s), 8.34 (3H br s).

(±)-3-Amino-1,1,1-trifluoro-2-methylpropan-2-ol (prepared as the free base by upscaling the above procedure and direct evaporation of the MeOH solution; 40 g, 280 mmol) and L-(+)-tartaric acid (42.0 g, 280 mmol) were dissolved in EtOH + 4% water (1398 mL), warmed to 65 °C over 30 min, and then left standing at RT for 16 h. The resultant solid was collected by filtration, dried, taken into EtOH + 4% water (384 mL), warmed to 80 °C, and then left standing at RT for 16 h. The resultant solid was collected by filtration, dried and taken into EtOH + 4% water (314 mL), warmed to 80 °C for 2 h and then left standing at RT for 16 h. The white solid was collected by filtration and dried to afford (S)-3-amino-1,1,1-trifluoro-2-methylpropan-2-ol **41** (+)-tartrate salt (18.4 g, 23%) ¹H NMR (D₂O) 1.31 (3H s), 3.05 (1H d *J* = 14.4), 3.19 (1H d *J* = 14.4), 4.35 (2H s). The absolute configuration was determined by X-ray crystallographic analysis of the free base (*vide infra*). The enantiomeric purity was determined via conversion to the Mosher's amide: tartrate salt **41** (1 mg) was dissolved in DCM (1 mL) and then DIPEA (6 μL) was added with sonication followed by (S)-α-methoxy-α-trifluoromethylphenylacetyl chloride (6 μL), and the mixture was analyzed directly by GC indicating 97.4% ee.

(S)-3-Amino-1,1,1-trifluoro-2-methylpropan-2-ol **41** (+)-tartrate salt (15.5 g, 52.9 mmol) was dissolved in MeOH (400 mL) and eluted through a column packed with SCX-2 ion-exchange resin (Isolute Si-propylsulfonic acid) with DCM/MeOH (9:1) until no more tartaric acid was detected in the eluent. The eluent was switched to NH₃-MeOH (9:1), and the combined eluent was evaporated to afford (S)-3-amino-1,1,1-trifluoro-2-methylpropan-2-ol **41** as a white crystalline solid (6.34 g, 70%). The absolute configuration was determined by single crystal X-ray analysis (Supporting Information Figure S2). ¹H NMR (DMSO-*d*₆) 1.21 (3H s), 1.45 (2H br s), 2.56 (1H d *J* = 13.4), 2.72 (1H d *J* = 13.4), 5.70 (1H br s).

HCl (1.5 M solution in MeOH, 30 mL) was added to a solution of (S)-3-amino-1,1,1-trifluoro-2-methylpropan-2-ol **41** (5 g, 34.9 mmol) in MeOH (30 mL) and the mixture was stirred at RT for 30 min. The solvent was evaporated, and the residue was recrystallized from MeCN to afford (S)-3-amino-1,1,1-trifluoro-2-methylpropan-2-ol **41** hydrochloride as a white solid (4.73 g, 75%). ¹H NMR (DMSO-*d*₆) 1.19 (3H s), 2.54 (1H d *J* = 13.4), 2.71 (1H d *J* = 13.4), 3.30 (3H br s), 5.80 (1H br s).

N-Methylmorpholine (0.413 mL, 4.18 mmol) was added to a solution of 3-amino-6-bromo-5-(trifluoromethyl)picolinic acid (0.397 g, 1.39 mmol), (±)-3-amino-1,1,1-trifluoro-2-methylpropan-2-ol hydrochloride **41** (0.250 g, 1.39 mmol), and HATU (0.529 g, 1.39 mmol) in DMF (10 mL). The reaction was stirred at RT for 3 h, poured into ice-water and extracted with EtOAc. The organic phase was washed with saturated aqueous NH₄Cl, dried (MgSO₄) and evaporated. Purification by flash column chromatography (30%-EtOAc-isohehexanes elution) afforded racemic 3-amino-6-bromo-N-(3,3,3-trifluoro-2-hydroxy-2-methylpropyl)-5-(trifluoromethyl)picolinamide (0.373 g, 65%), which was separated by preparative chiral SFC (Chiralpak OJ-H column, eluting with 12% [isopropanol + 0.1% DEA]/88% CO₂) to afford (S)-3-amino-6-bromo-N-(3,3,3-trifluoro-2-hydroxy-2-methylpropyl)-5-(trifluoromethyl)picolinamide **22** (0.119 g, 64%, >98% ee) as a beige solid, retention time 3.8 min with absolute stereochemistry confirmed by X-ray crystallography (Supporting Information, Figure S2). LRMS C₁₁H₁₀BrF₆N₃O₂ requires M⁺ 408.99, found [MH]⁺ 410.2. Elemental analysis requires C, 32.22%; H, 2.46%; N, 10.25% found C, 32.37 ± 0.00%; H, 2.43 ± 0.00%; N, 10.27 ± 0.04. ¹H NMR (DMSO-*d*₆) 1.24 (3H s), 3.45 (1H dd *J* = 13.8, 5.7), 3.68 (1H dd *J* = 13.8, 7.4), 6.29 (1H s), 7.30 (1H br s), 7.73 (1H s), 8.31 (1H t *J* = 6.5). ¹³C NMR (DMSO-*d*₆) 18.93 (q), 42.21 (t), 72.28 (s *J*_F = 26.6), 117.69 (s), 121.91 (s *J*_F = 273.2), 126.32 (s *J*_F = 285.8), 126.41 (d *J*_F = 5.2), 128.37 (s *J*_F = 32.0), 129.62 (s), 145.31 (s), 165.28 (s). ¹⁹F NMR (DMSO-*d*₆) -62.73 (s), -80.49 (s) and (R)-3-amino-6-bromo-N-(3,3,3-trifluoro-2-

hydroxy-2-methylpropyl)-5-(trifluoromethyl)picolinamide **23** (0.123 g, 66%, >98% ee), retention time 4.3 min. LRMS C₁₁H₁₀BrF₆N₃O₂ requires M⁺ 408.99, found [MH]⁺ 410.1. ¹H NMR (DMSO-*d*₆) 1.24 (3H s), 3.45 (1H dd *J* = 13.8, 5.7), 3.68 (1H dd *J* = 13.8, 7.4), 6.29 (1H s), 7.30 (1H br s), 7.73 (1H s), 8.31 (1H t *J* = 6.5).

3-Amino-6-bromo-N-(2-hydroxy-2-methylpropyl)-5-(trifluoromethyl)picolinamide (24). Prepared with the same procedure used for **17**, starting from 1-amino-2-methylpropan-2-ol and isolated as a yellow solid (0.300 g, 75%). LRMS C₁₁H₁₃BrF₃N₃O₂ requires M⁺ 355.01, found [MH]⁺ 356.1. ¹H NMR (DMSO-*d*₆) 1.10 (6H s), 3.24 (2H d *J* = 6.2), 4.70 (1H s), 7.30 (2H br s), 7.71 (1H s), 8.14 (1H t *J* = 6.1).

3-Amino-6-bromo-N-(3,3,3-trifluoro-2-hydroxy-2-(trifluoromethyl)propyl)-5-(trifluoromethyl)picolinamide (25). 2,2-Bis(trifluoromethyl)oxirane (0.500 g, 2.78 mmol) was added dropwise to a stirred mixture of 35% aq ammonia (1 mL, 18.1 mol) in Et₂O (1 mL). The biphasic reaction was stirred at RT for 3 h; the layers were separated and the aqueous phase was extracted twice with Et₂O. The combined organic phases were dried (MgSO₄) and evaporated to afford 2-(aminomethyl)-1,1,1,3,3,3-hexafluoropropan-2-ol as a white solid (0.355 g, 65%). ¹H NMR (DMSO-*d*₆) 3.03 (2H s), 3.15 (1H s), 4.23 (2H br s).

2-(Aminomethyl)-1,1,1,3,3,3-hexafluoropropan-2-ol (0.355 g, 1.80 mmol) was added to a solution of 3-amino-6-bromo-5-(trifluoromethyl)picolinic acid (0.428 g, 1.50 mmol) in NMP (6 mL) followed by HATU (0.571 g, 1.50 mmol). Triethylamine (0.209 mL, 1.50 mmol) was added; the reaction was stirred at RT for 30 min and then diluted with EtOAc and washed with 0.1 M aq NaOH, water, and brine. The organic phase was dried (MgSO₄), evaporated and purified by flash chromatography 0–20% EtOAc-isohehexane gradient to afford 3-amino-6-bromo-N-(3,3,3-trifluoro-2-hydroxy-2-(trifluoromethyl)propyl)-5-(trifluoromethyl)picolinamide **25** as a pale yellow solid (0.530 g, 76%). LRMS C₁₁H₇BrF₉N₃O₂ requires M⁺ 462.96, found [MH]⁺ 464.0. ¹H NMR (DMSO-*d*₆) 3.99 (2H d *J* = 6.5), 7.31 (2H br s), 7.74 (1H s), 8.31 (1H s), 8.49 (1H s).

(±)-3-Amino-N-(3,3,3-trifluoro-2-hydroxy-2-methylpropyl)-5-(trifluoromethyl)picolinamide (26). 2 M aq NaOH (2 M NaOH (0.182 mL, 4.54 mmol) was added to a solution of methyl 3-amino-5-(trifluoromethyl)picolinate **38** (0.998 g, 4.53 mmol) in MeOH (20 mL), and the reaction was stirred at RT for 30 min, then poured into water and adjusted to pH 1 with 1 M HCl. The product was extracted with EtOAc and the organic phase was washed with brine, dried (MgSO₄), and evaporated to afford 3-amino-5-(trifluoromethyl)picolinic acid **37** as an orange solid (0.850 g, 91%). ¹H NMR (DMSO-*d*₆) 7.08 (2H br s), 7.58 (1H d *J* = 1.5), 8.12 (1H d *J* = 1.5), 12.90 (1H br s).

3-Amino-1,1,1-trifluoro-2-methylpropan-2-ol (99 mg, 0.694 mmol) was added to a solution of 3-amino-5-(trifluoromethyl)picolinic acid (0.130 g, 0.631 mmol) in NMP (2 mL), followed by HATU (0.240 g, 0.631 mmol) and then dropwise addition of triethylamine (88 μL, 0.631 mmol). The reaction was stirred at RT for 16 h, then partitioned between 1 M aq NaOH and EtOAc. The organic phase was washed with brine, dried (MgSO₄) and evaporated. Purification by flash chromatography (0–80% EtOAc-isohehexanes gradient elution) afforded (±)-3-amino-N-(3,3,3-trifluoro-2-hydroxy-2-methylpropyl)-5-(trifluoromethyl)picolinamide **26** as a yellow oil (0.108 g, 52%). LRMS C₁₁H₁₁F₆N₃O₂ requires M⁺ 331.08, found [MH]⁺ 332.2. ¹H NMR (DMSO-*d*₆) 1.25 (3H s), 3.48 (1H dd *J* = 13.8, 7.3), 3.65 (1H dd *J* = 13.8, 7.3), 6.27 (1H s), 7.21 (2H br s), 7.56 (1H d *J* = 1.5), 8.11 (1H d *J* = 1.5), 8.12 (1H t *J* = 6.4).

(±)-3-Amino-6-methyl-N-(3,3,3-trifluoro-2-hydroxy-2-methylpropyl)-5-(trifluoromethyl)picolinamide (27). A suspension of methyl 3-amino-6-bromo-5-(trifluoromethyl)picolinate **39** (1.249 g, 4.18 mmol), methylboronic acid (0.250 g, 4.18 mmol), PdCl₂(dppf) (0.153 g, 0.209 mmol), and K₃PO₄ (2.66 g, 12.53 mmol) in toluene (10 mL) and water (5 mL) was heated in a sealed vial with microwave irradiation at 150 °C for 30 min. The reaction mixture was diluted with water and toluene and filtered and the phases separated. The aqueous phase was adjusted to pH 3 by addition of 2 M HCl and extracted twice with EtOAc. The combined organic phases were dried (MgSO₄),

evaporated and purified by flash chromatography (0–20% MeOH-DCM gradient elution) to afford 3-amino-6-methyl-5-(trifluoromethyl)picolinic acid **42** as a yellow oil (0.379 mg, 43%). LRMS $C_8H_7F_3N_2O_2$ requires M^+ 220.05, found $[MH]^+$ 221.0.

Triethylamine (0.190 mL, 1.363 mmol) was added to a solution of 3-amino-6-methyl-5-(trifluoromethyl)picolinic acid **42** (0.150 g, 0.681 mmol) in DCM (5 mL), followed by (\pm)-3-amino-1,1,1-trifluoro-2-methylpropan-2-ol hydrochloride **41** (0.122 g, 0.681 mmol) and HATU (0.285 g, 0.749 mmol). The reaction was stirred for 30 min at RT and then diluted with water. The phases were separated, and the organic phase was dried ($MgSO_4$), evaporated and purified by flash chromatography (0–100% EtOAc-isohexanes gradient elution) to afford (\pm)-3-amino-6-methyl-*N*-(3,3,3-trifluoro-2-hydroxy-2-methylpropyl)-5-(trifluoromethyl)picolinamide **27** as a yellow solid (0.175 g, 70%). LRMS $C_{12}H_{15}F_6N_3O_2$ requires M^+ 345.09, found $[MH]^+$ 346.1. 1H NMR ($CDCl_3$) 1.43 (3H s), 2.58 (3H s), 3.68 (1H dd J = 14.5, 7.1), 3.78 (1H dd J = 14., 6.2), 4.57 (1H s), 5.99 (2H br s), 8.53 (1H s), 7.30 (1H s).

(*ent*-1)-3-Amino-6-ethyl-*N*-(3,3,3-trifluoro-2-hydroxy-2-methylpropyl)-5-(trifluoromethyl)picolinamide (**28a**) and (*ent*-2)-3-Amino-6-ethyl-*N*-(3,3,3-trifluoro-2-hydroxy-2-methylpropyl)-5-(trifluoromethyl)picolinamide (**28b**). Acetylacetone (7.06 mL, 60.2 mmol) was added to a suspension of methyl 3-amino-6-bromo-5-(trifluoromethyl)picolinate **39** (15 g, 50.2 mmol) in toluene (60 mL), followed by *p*-toluenesulfonic acid (0.954 g, 5.02 mmol). The suspension was heated at reflux with a Dean–Stark trap for 5 h. After cooling, the reaction mixture was partitioned between EtOAc and saturated $NaHCO_3$, and the combined organic phases were washed with brine, dried ($MgSO_4$) and evaporated. Purification by flash chromatography (0–80% EtOAc-isohexane gradient elution) afforded methyl 6-bromo-3-(2,5-dimethyl-1*H*-pyrrol-1-yl)-5-(trifluoromethyl)picolinate **43** as a yellow solid (14.9 g, 79%). 1H NMR ($DMSO-d_6$) 1.90 (6H s), 3.68 (3H s), 5.89 (2H s), 8.51 (1H s).

One molar aq Cs_2CO_3 (1.67 mL, 1.67 mmol) was added to a suspension of methyl 6-bromo-3-(2,5-dimethyl-1*H*-pyrrol-1-yl)-5-(trifluoromethyl)picolinate **43** (0.923 g, 2.47 mmol), ethylboronic acid (0.181 g, 2.447 mmol), and $PdCl_2(dppf)$ (0.200 g, 0.245 mmol) in THF (5 mL). The reaction was heated in a sealed vial with microwave irradiation at 150 °C for 15 min. The reaction mixture was filtered through Celite and washed with EtOAc, and the filtrate was washed with water, brine, dried ($MgSO_4$) and evaporated. Flash chromatography (0–80% EtOAc-isohexane gradient elution) afforded an inseparable mixture of **43** and methyl 3-(2,5-dimethyl-1*H*-pyrrol-1-yl)-6-ethyl-5-(trifluoromethyl)picolinate **44** in approximately 1:1 ratio based on UV absorbance (0.492 g, ~22%). LRMS $C_{16}H_{17}F_3N_2O_2$ requires M^+ 326.12, found $[MH]^+$ 327.2.

The above mixture (0.492 g, approximately 1.508 mmol) was taken into THF (10 mL) and 2 M aq NaOH (66 μ L, 1.508 mmol), and the reaction mixture was stirred at RT for 1 h. Water was added, and the solution was adjusted to pH 4 with 1 M HCl and extracted with EtOAc. The combined organic phases were washed with brine, dried ($MgSO_4$) and evaporated to afford a brown viscous oil (0.482 g) corresponding to 15% by UV peak area 3-(2,5-dimethyl-1*H*-pyrrol-1-yl)-6-ethyl-5-(trifluoromethyl)picolinic acid. LRMS $C_{15}H_{15}F_3N_2O_2$ requires M^+ 312.11, found $[MH]^+$ 313.2.

The above crude material (0.482 g) was taken into NMP (2 mL). (\pm)-3-Amino-1,1,1-trifluoro-2-methylpropan-2-ol hydrochloride **41** (0.243 g, 1.698 mmol) was added, followed by HATU (0.646 g, 1.698 mmol) and triethylamine (0.473 mL, 3.40 mmol). The reaction was stirred at RT for 16 h and then partitioned between EtOAc and 1 M NaOH. The organic phase was washed with brine, dried ($MgSO_4$), evaporated and partially purified by mass-directed preparative LCMS to afford 3-(2,5-dimethyl-1*H*-pyrrol-1-yl)-6-ethyl-*N*-(3,3,3-trifluoro-2-hydroxy-2-methylpropyl)-5-(trifluoromethyl)picolinamide **45** as a brown viscous oil in 67% purity by UV peak area (0.146 g, approx 21%). LRMS $C_{13}H_{15}F_6N_3O_2$ requires M^+ 453.19, found M^+ 453.3.

Triethylamine (93 μ L, 0.668 mmol) was added to 3-(2,5-dimethyl-1*H*-pyrrol-1-yl)-6-ethyl-*N*-(3,3,3-trifluoro-2-hydroxy-2-methylpropyl)-5-(trifluoromethyl)picolinamide **45** (0.146 g, 0.334 mmol) in EtOH (5 mL) and water (5 mL), followed by hydroxylamine

hydrochloride (0.232 g, 3.34 mmol). The mixture was heated at reflux for 10 h and then partitioned between 1 M HCl and EtOAc. The organic phase was washed with brine, dried ($MgSO_4$) and evaporated. The crude product was purified by mass-directed preparative LCMS to afford (\pm)-3-amino-6-ethyl-*N*-(3,3,3-trifluoro-2-hydroxy-2-methylpropyl)-5-(trifluoromethyl)picolinamide as a pale yellow solid (23 mg, 19%). The racemic mixture was separated by preparative chiral SFC (Chiralcel OD-H column eluting with 15% 2-propanol + 0.1% v/v diethylamine/85% CO_2) to afford (*ent*-1)-3-amino-6-ethyl-*N*-(3,3,3-trifluoro-2-hydroxy-2-methylpropyl)-5-(trifluoromethyl)picolinamide **28a** as an off-white solid (5 mg), retention time 4.03 min. LRMS $C_{13}H_{15}F_6N_3O_2$ requires M^+ 359.11, found $[MH]^+$ 360.2. 1H NMR ($DMSO-d_6$) 1.24 (3H t J = 7.4), 1.26 (3H s), 2.75 (2H q J = 7.3), 3.48 (1H dd J = 13.8, 5.6), 3.66 (1H dd J = 13.8, 7.2), 6.32 (1H s), 6.97 (2H br s), 7.56 (1H s), 8.50 (1H t J = 6.3) and (*ent*-2)-3-amino-6-ethyl-*N*-(3,3,3-trifluoro-2-hydroxy-2-methylpropyl)-5-(trifluoromethyl)picolinamide **28b** as an off-white solid (4 mg), retention time 4.59 min. LRMS $C_{13}H_{15}F_6N_3O_2$ requires M^+ 359.11, found $[MH]^+$ 360.2. 1H NMR ($DMSO-d_6$) 1.24 (3H t J = 7.4), 1.26 (3H s), 2.75 (2H q J = 7.3), 3.48 (1H dd J = 13.8, 5.6), 3.66 (1H dd J = 13.8, 7.2), 6.32 (1H s), 6.97 (2H br s), 7.56 (1H s), 8.50 (1H t J = 6.3).

(*S*)-3-Amino-*N*-(3,3,3-trifluoro-2-hydroxy-2-methylpropyl)-5,6-bis(trifluoromethyl)picolinamide (**29**). Nine microwave reactions were conducted in batch format as follows: (trifluoromethyl)-trimethylsilane (2.49 mL, 15.91 mmol) was added to a mixture of potassium fluoride (0.462 g, 7.95 mmol), copper(I) iodide (1.52 g, 7.95 mmol) and methyl 6-bromo-3-(2,5-dimethyl-1*H*-pyrrol-1-yl)-5-(trifluoromethyl)picolinate **43** (2.0 g, 5.30 mmol) in a microwave vial. The reaction was irradiated at 100 °C for 3 h, and then the 9 crude reaction mixtures were combined for work up by adding cautiously to 5 M aqueous ammonia and extracting three times with EtOAc. The combined organic phases were further washed sequentially with 5 M aqueous ammonia, 1 M HCl, saturated $NaHCO_3$ then brine and dried ($MgSO_4$). Following evaporation, flash chromatography (0–10% EtOAc gradient elution) gave a brown oil which partly crystallized on standing. The supernatant oil was decanted and discarded to afford methyl 3-(2,5-dimethyl-1*H*-pyrrol-1-yl)-5,6-bis(trifluoromethyl)picolinate **46** as yellow crystals (5.7 g, 33%). LRMS $C_{15}H_{12}F_6N_2O_2$ requires M^+ 366.08, found $[MH]^+$ 367.0. 1H NMR ($DMSO-d_6$) 1.84 (6H s), 3.63 (3H s), 5.80 (2H s), 8.74 (1H s).

One molar NaOH (31 mL 31.1 mmol) was added to a solution of methyl 3-(2,5-dimethyl-1*H*-pyrrol-1-yl)-5,6-bis(trifluoromethyl)picolinate **46** (5.70 g, 15.6 mmol) in MeOH (90 mL). The reaction was stirred at RT for 1 h, and the MeOH was evaporated. The residue was adjusted to pH 3 with 1 M HCl and then extracted three times with EtOAc. The combined organic phases were washed with brine, dried ($MgSO_4$) and evaporated to afford 3-(2,5-dimethyl-1*H*-pyrrol-1-yl)-5,6-bis(trifluoromethyl)picolinic acid containing 1 equiv EtOAc as a brown oil (2.96 g, 54%). LRMS $C_{14}H_{10}F_6N_2O_2$ requires M^+ 352.06, found $[MH]^+$ 353.0. 1H NMR ($DMSO-d_6$) 1.94 (6H s) 5.86 (2H s), 8.71 (1H s), 14.3 (1H br s).

Hydroxylamine hydrochloride (5.84 g, 84.0 mmol) was added to a solution of 3-(2,5-dimethyl-1*H*-pyrrol-1-yl)-5,6-bis(trifluoromethyl)picolinic acid (2.96 g, 8.40 mmol) in 2:1 EtOH-water (30 mL), followed by triethylamine (2.34 mL, 16.8 mmol). The reaction was heated at 100 °C for 3 h, and the solvent was evaporated. The residue was diluted with water and extracted three times with EtOAc. The combined organic phases were washed with brine, dried ($MgSO_4$) and evaporated. The crude product was purified first by normal phase column chromatography (75–100% EtOAc-isohexanes gradient elution) and then by reverse phase chromatography (C18 column; 10–95% MeCN-water gradient elution, each containing 1% HCl) to afford 3-amino-5,6-bis(trifluoromethyl)picolinic acid hydrochloride **47** as a yellow solid (1.95 g, 73%). LRMS $C_8H_4F_6N_2O_2$ requires M^+ 274.02, found $[MH]^+$ 275.2. 1H NMR ($DMSO-d_6$) 7.59 (2H br s), 7.80 (1H s), 13.30 (1H br s).

(*S*)-3-Amino-1,1,1-trifluoro-2-methylpropan-2-ol hydrochloride **41** (1 g, 5.57 mmol) was added to a solution of 3-amino-5,6-bis(trifluoromethyl)picolinic acid hydrochloride **47** (1.5 g, 5.47 mmol) in DMF (61 mL) followed by HATU (2.497 g, 6.57 mmol),

and then diisopropylethylamine (3.81 mL, 22.28 mmol) was added in ~0.5 mL portions every 5–10 min over a total of 1 h. The reaction mixture was added to water and extracted with EtOAc, and the organic phase was washed with 1 M HCl, 2 M NaOH, water, and brine and dried (MgSO₄). Evaporation and flash chromatography (0–30% EtOAc-isohexanes gradient elution) afforded an oil, which was taken into hot DCM and isohexane was added until the solution became turbid. On cooling, filtration afforded (S)-3-amino-N-(3,3,3-trifluoro-2-hydroxy-2-methylpropyl)-5-bis(trifluoromethyl)picolinamide **29** as a white solid (1.67 g, 75%). LRMS C₁₂H₁₀F₉N₃O₂ requires M⁺ 399.06, found [MH]⁺ 400.1. Elemental analysis requires C, 36.10%; H, 2.52%; N, 10.53% found C, 36.20 ± 0.02%; H, 2.49 ± 0.06%; N, 10.56 ± 0.05%. ¹H NMR (DMSO-*d*₆) 1.25 (3H s), 3.49 (1H dd *J* = 14.0, 5.6), 3.67 (1H dd *J* = 13.8, 7.3), 6.33 (1H s), 7.79 (1H s), 7.80 (2H br s), 8.31 (1H t *J* = 6.4). ¹³C NMR (DMSO-*d*₆) 18.95 (q), 42.21 (t), 72.14 (s *J*_F = 27), 129.87 (s *J*_F = 272), 121.97 (s *J*_F = 272), 124.28 (d *J*_F = 6), 26.19 (s *J*_F = 36), 126.32 (s *J*_F = 287), 126.34 (s *J*_F = 34), 127.85 (s), 147.78 (s), 165.22 (s). ¹⁹F NMR (DMSO-*d*₆) –59.81 (q *J* = 11), –61.92 (q *J* = 11), 80.49 (s).

(ent-1)-3-Amino-6-(methylamino)-N-(3,3,3-trifluoro-2-hydroxy-2-methylpropyl)-5-(trifluoromethyl)picolinamide (30a) and (ent-2)-3-Amino-6-(methylamino)-N-(3,3,3-trifluoro-2-hydroxy-2-methylpropyl)-5-(trifluoromethyl)picolinamide (30b). Two molar eq NaOH (2.52 mL, 5.04 mmol) was added to a solution of methyl 6-bromo-3-(2,5-dimethyl-1H-pyrrol-1-yl)-5-(trifluoromethyl)picolinate **43** (1.9 g, 1.504 mmol) in THF (10 mL). The reaction was stirred at RT for 1 h, then poured into water, adjusted to pH 4 with 1 M HCl and extracted twice with EtOAc. The combined organic phases were washed with brine, dried (MgSO₄), and evaporated to afford crude 6-bromo-3-(2,5-dimethyl-1H-pyrrol-1-yl)-5-(trifluoromethyl)picolinic acid **48** as an orange solid (1.78 g, 97%). LRMS C₁₃H₁₀BrF₃N₃O₂ requires M⁺ 361.99, found [MH]⁺ 363.1. ¹H NMR (DMSO-*d*₆) 1.92 (6H s), 5.74 (2H s), 8.14 (1H s), 14.3 (1H br s).

Methylamine (2 M THF, 0.826 mL, 1.652 mmol) was added to a solution of 6-bromo-3-(2,5-dimethyl-1H-pyrrol-1-yl)-5-(trifluoromethyl)picolinic acid **48** (0.300 g, 0.826 mmol) in THF (1 mL). The reaction was stirred at RT for 10 days, then partitioned between 0.5 M HCl and EtOAc. The organic phase was washed with brine, dried (MgSO₄), and evaporated to afford crude 3-(2,5-dimethyl-1H-pyrrol-1-yl)-6-(methylamino)-5-(trifluoromethyl)picolinic acid as a red oil (0.240 g, 92%). LRMS C₁₄H₁₄F₃N₃O₂ requires M⁺ 313.10, found [MH]⁺ 314.2. ¹H NMR (DMSO-*d*₆) 1.89 (6H s), 2.92 (3H d *J* = 4.3), 5.72 (2H s), 7.03 (1H q *J* = 4.2), 7.72 (1H s), 13.3 (1H br s).

HATU (0.320 g, 0.843 mmol) was added to a solution of 3-(2,5-dimethyl-1H-pyrrol-1-yl)-6-(methylamino)-5-(trifluoromethyl)picolinic acid (0.240 g, 0.766 mmol) and (±)-3-amino-1,1,1-trifluoro-2-methylpropan-2-ol hydrochloride **41** (0.121 g, 0.843 mmol) in NMP (1 mL) followed by triethylamine (0.214 mL, 1.532 mmol). The reaction was stirred at RT for 16 h then partitioned between EtOAc and 1 M NaOH. The organic phase was washed with brine, dried (MgSO₄) and evaporated to afford crude 3-(2,5-dimethyl-1H-pyrrol-1-yl)-6-(methylamino)-N-(3,3,3-trifluoro-2-hydroxy-2-methylpropyl)-5-(trifluoromethyl)picolinamide (0.174 g, 52%). LCMS C₁₈H₂₀F₆N₄O₂ requires M⁺ 438.15, found [MH]⁺ 439.3.

Hydroxylamine hydrochloride (0.269 g, 3.88 mmol) was added to a solution of 3-(2,5-dimethyl-1H-pyrrol-1-yl)-6-(methylamino)-N-(3,3,3-trifluoro-2-hydroxy-2-methylpropyl)-5-(trifluoromethyl)picolinamide (0.170 g, 0.388 mmol) in EtOH (5 mL) and water (3 mL), followed by triethylamine (0.108 mL, 0.776 mmol). The mixture was heated at reflux for 10 h and stood at RT for 16 h. The reaction was partitioned between 1 M HCl/EtOAc and the organic phase was washed with brine, dried (MgSO₄), and evaporated. Flash chromatography (0–60% EtOAc-isohexanes gradient elution) afforded (±)-3-amino-6-(methylamino)-N-(3,3,3-trifluoro-2-hydroxy-2-methylpropyl)-5-(trifluoromethyl)picolinamide which was separated by preparative chiral SFC (Chiralpak OJ-H column, eluting with 10%–50% [MeOH + 0.1% diethylamine]-CO₂ gradient to afford (ent-1)-3-amino-6-(methylamino)-N-(3,3,3-trifluoro-2-hydroxy-2-methylpropyl)-5-(trifluoromethyl)picolinamide **30a** as a colorless oil (25 mg, 36%), retention time 3.22 min. LRMS C₁₂H₁₄F₆N₄O₂ requires M⁺ 360.1,

found [MH]⁺ 361.2. ¹H NMR (DMSO-*d*₆) 1.27 (3H s), 2.82 (3H d *J* = 4.5), 3.45 (1H dd *J* = 13.8, 5.6), 3.64 (1H dd *J* = 13.8, 7.3), 5.90 (1H q *J* = 4.6), 6.22 (2H br s), 6.32 (1H s), 7.48 (1H s), 8.50 (1H t *J* = 6.4) and (ent-2)-3-amino-6-(methylamino)-N-(3,3,3-trifluoro-2-hydroxy-2-methylpropyl)-5-(trifluoromethyl)picolinamide **30b** as a colorless oil (24 mg, 34%), retention time 4.01 min. LRMS C₁₂H₁₄F₆N₄O₂ requires M⁺ 360.1, found [MH]⁺ 361.2. ¹H NMR (DMSO-*d*₆) 1.27 (3H s), 2.82 (3H d *J* = 4.5), 3.45 (1H dd *J* = 13.8, 5.6), 3.64 (1H dd *J* = 13.8, 7.3), 5.90 (1H q *J* = 4.6), 6.22 (2H br s), 6.32 (1H s), 7.48 (1H s), 8.50 (1H t *J* = 6.4).

(ent-1)-3-Amino-6-(dimethylamino)-N-(3,3,3-trifluoro-2-hydroxy-2-methylpropyl)-5-(trifluoromethyl)picolinamide (31a) and (ent-2)-3-Amino-6-(dimethylamino)-N-(3,3,3-trifluoro-2-hydroxy-2-methylpropyl)-5-(trifluoromethyl)picolinamide (31b). Dimethylamine (0.209 mL, 1.652 mmol) was added to solution of 6-bromo-3-(2,5-dimethyl-1H-pyrrol-1-yl)-5-(trifluoromethyl)picolinic acid **48** (0.300 g, 0.826 mmol), and the reaction was stirred at RT for 72 h and then partitioned between 0.5 M HCl and EtOAc. The organic phase was washed with brine, dried (MgSO₄) and evaporated to afford crude 3-(2,5-dimethyl-1H-pyrrol-1-yl)-6-(dimethylamino)-5-(trifluoromethyl)picolinic acid as an orange oil (0.151 g, 56%) LRMS C₁₅H₁₆F₃N₃O₂ requires M⁺ 327.12, found [MH]⁺ 328.2.

HATU (0.193 g, 0.507 mmol) was added to a solution of 3-(2,5-dimethyl-1H-pyrrol-1-yl)-6-(dimethylamino)-5-(trifluoromethyl)picolinic acid (0.151 g, 0.461 mmol) and (±)-3-amino-1,1,1-trifluoro-2-methylpropan-2-ol hydrochloride **41** (73 mg, 0.507 mmol) in NMP (1 mL) followed by triethylamine (0.129 mL, 0.923 mmol). The reaction was stirred at RT for 16 h and then partitioned between EtOAc and 1 M NaOH. The organic phase was washed with brine, dried (MgSO₄) and evaporated to afford crude 3-(2,5-dimethyl-1H-pyrrol-1-yl)-6-(dimethylamino)-N-(3,3,3-trifluoro-2-hydroxy-2-methylpropyl)-5-(trifluoromethyl)picolinamide as an orange oil (0.165 g, 78%) LRMS C₁₉H₂₂F₆N₄O₂ requires M⁺ 452.16, found [MH]⁺ 453.3.

Hydroxylamine hydrochloride (0.253 g, 3.65 mmol) was added to a solution of 3-(2,5-dimethyl-1H-pyrrol-1-yl)-6-(dimethylamino)-N-(3,3,3-trifluoro-2-hydroxy-2-methylpropyl)-5-(trifluoromethyl)picolinamide (0.165 g, 0.365 mmol) in EtOH (10 mL) and water (5 mL), followed by triethylamine (0.102 mL, 0.729 mmol). The mixture was heated at reflux for 6 h. The reaction was partitioned between 1 M HCl/EtOAc, and the organic phase was washed with brine, dried (MgSO₄), and evaporated. Flash chromatography (0–60% EtOAc-isohexane gradient elution) afforded 3-amino-6-(dimethylamino)-N-(3,3,3-trifluoro-2-hydroxy-2-methylpropyl)-5-(trifluoromethyl)picolinamide, which was separated by preparative chiral SFC (Chiralcel OD-H column; 12% [2-propanol + 0.1% DEA]/88% CO₂ elution) to afford (ent-1)-3-amino-6-(dimethylamino)-N-(3,3,3-trifluoro-2-hydroxy-2-methylpropyl)-5-(trifluoromethyl)picolinamide **31a** as a colorless glassy solid (25 mg, 36%), retention time 4.09 min. LRMS C₁₃H₁₆F₆N₄O₂ requires M⁺ 374.12, found [MH]⁺ 375.3. ¹H NMR (DMSO-*d*₆) 1.26 (3H s), 2.67 (6H s), 3.48 (1H dd *J* = 13.8, 5.6), 3.64 (1H dd *J* = 13.8, 7.2), 6.32 (1H s), 6.79 (2H br s), 7.60 (1H s), 8.31 (1H t *J* = 6.4) and (ent-2)-3-amino-6-(dimethylamino)-N-(3,3,3-trifluoro-2-hydroxy-2-methylpropyl)-5-(trifluoromethyl)picolinamide **31b** as a colorless glassy solid (25 mg, 36%), retention time 4.74 min. LRMS C₁₃H₁₆F₆N₄O₂ requires M⁺ 374.12, found [MH]⁺ 375.3. ¹H NMR (DMSO-*d*₆) 1.26 (3H s), 2.67 (6H s), 3.48 (1H dd *J* = 13.8, 5.6), 3.64 (1H dd *J* = 13.8, 7.2), 6.32 (1H s), 6.79 (2H br s), 7.60 (1H s), 8.31 (1H t *J* = 6.4).

(S)-3-Amino-6-ethoxy-N-(3,3,3-trifluoro-2-hydroxy-2-methylpropyl)-5-(trifluoromethyl)picolinamide (32). Two molar NaOH (135 mL, 270 mmol) was added to a solution of methyl 6-bromo-3-(2,5-dimethyl-1H-pyrrol-1-yl)-5-(trifluoromethyl)picolinate **43** (34 g, 90 mmol) in MeOH (460 mL), and the reaction was heated at 90 °C for 3 h. The solvent was evaporated, and the residue was adjusted to pH 1 with 2 M HCl and extracted twice with EtOAc. The combined organic phases were washed with brine, dried (MgSO₄), and evaporated to afford 3-(2,5-dimethyl-1H-pyrrol-1-yl)-6-methoxy-5-(trifluoromethyl)picolinic acid **49** as a reddish-brown solid (28.2 g, 100%). LRMS C₁₄H₁₃F₃N₂O₃ requires M⁺ 314.09, found [MH]⁺ 315.2.

¹H NMR (DMSO-*d*₆) 1.90 (6H s), 4.07 (3H s), 5.77 (2H s), 8.19 (1H s), 13.8 (1H br s).

Conc H₂SO₄ (42 μL, 0.795 mmol) was added to a solution of 3-(2,5-dimethyl-1H-pyrrol-1-yl)-6-methoxy-5-(trifluoromethyl)picolinic acid **49** (500 mg, 1.591 mmol) in MeOH (16 mL). The reaction was heated at reflux for 20 h, and then the solvent was evaporated. The residue was adjusted to pH 7 with sat. NaHCO₃ and extracted with EtOAc. The organic phase was washed with brine, dried (MgSO₄), and purified by flash chromatography (0–10% EtOAc-isohehexane gradient) to afford methyl 3-(2,5-dimethyl-1H-pyrrol-1-yl)-6-methoxy-5-(trifluoromethyl)picolinate as an off-white solid (0.391 g, 75%). LRMS C₁₅H₁₃F₃N₂O₃ requires M⁺ 328.10, found [MH]⁺ 329.2. ¹H NMR (DMSO-*d*₆) 1.89 (6H s), 3.64 (3H s), 4.07 (3H s), 5.80 (2H s), 8.29 (1H s).

KI (0.589 g, 3.55 mmol) was added to a solution of methyl 3-(2,5-dimethyl-1H-pyrrol-1-yl)-6-methoxy-5-(trifluoromethyl)picolinate (0.291 g, 0.886 mmol) in MeCN (9 mL) followed by TMSCl (0.453 mL, 3.54 mmol). The reaction was heated at reflux for 5 h, and then the solvent was evaporated. The residue was taken into EtOAc, washed with water then brine and dried (MgSO₄). Evaporation and partial purification by flash chromatography (0–30% EtOAc-isohehexanes gradient elution) afforded crude methyl 3-(2,5-dimethyl-1H-pyrrol-1-yl)-6-hydroxy-5-(trifluoromethyl)picolinate as a white solid (0.176 g, 54%). LRMS C₁₄H₁₃F₃N₂O₃ requires M⁺ 314.09, found [MH]⁺ 315.4.

Triphenylphosphine (0.250 g, 0.952 mmol) was added to a solution of methyl 3-(2,5-dimethyl-1H-pyrrol-1-yl)-6-hydroxy-5-(trifluoromethyl)picolinate (0.176 g, 0.476 mmol) in dioxane (5 mL), followed by EtOH (0.6 mL, 10.28 mmol) and dropwise addition of DEAD (0.151 mL, 0.952 mmol). The reaction was stirred at RT for 2 h and the solvent was evaporated. Purification by flash chromatography (0–10% EtOAc-isohehexanes gradient elution) afforded ethyl 3-(2,5-dimethyl-1H-pyrrol-1-yl)-6-ethoxy-5-(trifluoromethyl)picolinate **50** as a colorless viscous oil (0.100 g, 61%). LRMS C₁₆H₁₇F₃N₂O₃ requires M⁺ 342.12, found [MH]⁺ 343.2. ¹H NMR (DMSO-*d*₆) 1.38 (3H t J = 7.1), 1.88 (6H s), 3.63 (3H s), 4.52 (2H q J = 7.1), 5.79 (2H s), 8.27 (1H s).

Two molar NaOH (0.613 mL, 1.226 mmol) was added to a solution of ethyl 3-(2,5-dimethyl-1H-pyrrol-1-yl)-6-ethoxy-5-(trifluoromethyl)picolinate **50** (0.140 g, 0.409 mmol) in THF (2 mL). The reaction was heated at reflux for 6 h and the solvent was evaporated. The residue was acidified to pH 1 with 5 M HCl and extracted with EtOAc. The organic phase was washed with brine, dried (MgSO₄) and evaporated to afford crude 3-(2,5-dimethyl-1H-pyrrol-1-yl)-6-ethoxy-5-(trifluoromethyl)picolinic acid as a yellow oil (35 mg, 26%). LRMS C₁₅H₁₅F₃N₂O₃ requires M⁺ 328.10, found [MH]⁺ 329.2.

HATU (49 mg, 0.128 mmol) was added to a solution of 3-(2,5-dimethyl-1H-pyrrol-1-yl)-6-ethoxy-5-(trifluoromethyl)picolinic acid (35 mg, 0.107 mmol) and (S)-3-amino-1,1,1-trifluoro-2-methylpropan-2-ol hydrochloride **41** (19 mg, 0.107 mmol) in DMF (1 mL) followed by DIPEA (56 μL, 0.320 mmol). The reaction was stirred at RT for 3 h then partitioned between EtOAc and water. The organic phase was washed with 1 M HCl, 2 M NaOH, brine and then dried (MgSO₄). Evaporation afforded crude 3-(2,5-dimethyl-1H-pyrrol-1-yl)-6-ethoxy-N-(3,3,3-trifluoro-2-hydroxy-2-methylpropyl)-5-(trifluoromethyl)picolinamide as a yellow oil (43 mg, 89%). LRMS C₁₉H₂₁F₆N₃O₃ requires M⁺ 453.15, found [MH]⁺ 454.3.

Hydroxylamine hydrochloride (66 mg, 0.948 mmol) was added to a solution of 3-(2,5-dimethyl-1H-pyrrol-1-yl)-6-ethoxy-N-(3,3,3-trifluoro-2-hydroxy-2-methylpropyl)-5-(trifluoromethyl)picolinamide (43 mg, 0.095 mmol) in EtOH (0.6 mL) and water (0.3 mL), followed by triethylamine (40 μL, 0.285 mmol), and the mixture was heated at reflux for 5 h. The reaction was partitioned between water/EtOAc then organic phase was washed with brine, dried (MgSO₄) and evaporated. Purification by preparative HPLC (C18 column, 50–95% [MeCN + 0.1% DEA] – [water + 0.1% DEA] gradient) afforded (S)-3-amino-6-ethoxy-N-(3,3,3-trifluoro-2-hydroxy-2-methylpropyl)-5-(trifluoromethyl)picolinamide **32** as a white solid (13 mg, 37%). LRMS C₁₃H₁₅F₆N₃O₃ requires M⁺ 375.10, found [MH]⁺ 376.1. ¹H NMR (DMSO-*d*₆) 1.25 (3H s), 1.32 (3H t J = 7.0), 3.46 (1H dd J = 13.7, 5.5),

3.65 (1H dd J = 13.6, 7.2), 4.38 (2H q J = 7.0), 6.29 (1H s), 6.67 (1H s), 7.67 (1H s) 8.26 (1H t J = 6.2).

(S)-3-Amino-6-methoxy-N-(3,3,3-trifluoro-2-hydroxy-2-methylpropyl)-5-(trifluoromethyl)picolinamide (**33**). Triethylamine (37.5 mL, 269 mmol) was added to 3-(2,5-dimethyl-1H-pyrrol-1-yl)-6-methoxy-5-(trifluoromethyl)picolinic acid **49** (28.2 g, 90 mmol) in EtOH (540 mL) and water (270 mL) followed by hydroxylamine hydrochloride (62.4 g, 897 mmol). The reaction was heated at 100 °C for 5 h and then partitioned between EtOAc (800 mL) and 1 M HCl (800 mL). The aqueous phase was extracted with EtOAc (800 mL) and the combined organic phases were washed with brine, dried (MgSO₄) and evaporated. The foregoing procedure was repeated analogously starting from 3-(2,5-dimethyl-1H-pyrrol-1-yl)-6-methoxy-5-(trifluoromethyl)picolinic acid (75.7 g, 241 mmol) and the crude products from both reactions were combined and recrystallized from isohehexanes with hot filtration to afford 3-amino-6-methoxy-5-(trifluoromethyl)picolinic acid **51** in 3 crops as an orange/yellow solid (41.59 g, 53%). LRMS C₈H₇F₃N₂O₃ requires M⁺ 236.04, found [MH]⁺ 237.1. ¹H NMR (DMSO-*d*₆) 3.90 (3H s), 7.68 (1H s), 7.80–9.20 (3H br s).

DIPEA (62.4 g, 897 mmol) was added to a solution of 3-amino-6-methoxy-5-(trifluoromethyl)picolinic acid **51** (22.0 g, 93 mmol) and (S)-3-amino-1,1,1-trifluoro-2-methylpropan-2-ol **41** hydrochloride (16.73 g, 93 mmol) in NMP (800 mL), followed by HATU (42.5 g, 112 mmol). The reaction was stirred for 1 h at RT, added to EtOAc (4 L) and then washed with 1 M NaOH (2 × 2 L), water (2 L) and brine (2 L) and dried (MgSO₄) and evaporated to afford a brown oil. The foregoing procedure was repeated analogously starting from 3-amino-6-methoxy-5-(trifluoromethyl)picolinic acid **51** (14.0 g, 59.3 mmol), and the crude products from both reactions were combined and initially purified by flash chromatography (5–100% EtOAc-isohehexane gradient elution). The resultant solid was dissolved in the minimum volume of hot DCM, which on cooling reprecipitated. Filtration and drying afforded (S)-3-amino-6-methoxy-N-(3,3,3-trifluoro-2-hydroxy-2-methylpropyl)-5-(trifluoromethyl)picolinamide **33** as a white solid (33.6 g, 59%). LRMS C₁₂H₁₃F₆N₃O₃ requires M⁺ 361.08, found [MH]⁺ 362.2. Elemental analysis requires C, 39.90%; H, 3.63%; N, 11.63% found C, 40.22 ± 0.06%; H, 3.68 ± 0.11%; N, 11.76 ± 0.04%. ¹H NMR (DMSO-*d*₆) 1.26 (3H s), 3.46 (1H dd J = 13.3, 5.6), 3.66 (1H dd J = 13.7, 7.3), 3.92 (3H s), 6.29 (1H s), 6.69 (2H br s), 7.68 (1H s), 8.30 (1H t J = 6.4). ¹³C NMR (DMSO-*d*₆) 18.95 (q), 42.19 (t), 53.56 (q), 72.27 (s J_F = 26.8), 116.07 (s J_F = 32.3), 122.40 (s J_F = 272.1), 124.85 (s), 126.43 (s J_F = 287.1), 128.29 (d J_F = 5.2), 141.0 (s), 148.51 (s), 166.3 (s). ¹⁹F NMR (DMSO-*d*₆) –62.71 (s), –80.46 (s).

■ ASSOCIATED CONTENT

Supporting Information

The Supporting Information is available free of charge at <https://pubs.acs.org/doi/10.1021/acs.jmedchem.1c00343>.

Molecular formula strings for final compounds (CSV)

X-ray crystallographic data for compounds **22** and **41**; list of off-target safety profiling assays; CFTR HBEC ion transport assay additional experimental information; experimental procedures for *in vitro* and *in vivo* pharmacokinetic and metabolite ID studies together with *in vitro* plasma protein binding studies; experimental details and toxicokinetic data for exploratory toxicology studies on compounds **22** and **33**; characterization data on final compounds **6–33** (PDF)

■ AUTHOR INFORMATION

Corresponding Author

David A. Sandham – Novartis Institutes for Biomedical

Research, Cambridge, Massachusetts 02139, United States;

orcid.org/0000-0003-4523-9931;

Email: david.sandham@novartis.com

Authors

Darren Le Grand – Novartis Institutes for Biomedical Research, Horsham Research Center, Horsham RH12 SAB, U.K.
Martin Gosling – Novartis Institutes for Biomedical Research, Horsham Research Center, Horsham RH12 SAB, U.K.
Urs Baettig – Novartis Institutes for Biomedical Research, Horsham Research Center, Horsham RH12 SAB, U.K.
Parmjit Bahra – Novartis Institutes for Biomedical Research, Horsham Research Center, Horsham RH12 SAB, U.K.
Kamlesh Bala – Novartis Institutes for Biomedical Research, Horsham Research Center, Horsham RH12 SAB, U.K.
Cara Brocklehurst – Novartis Institutes for Biomedical Research, Basel CH 4002, Switzerland; orcid.org/0000-0002-0484-5540
Emma Budd – Novartis Institutes for Biomedical Research, Horsham Research Center, Horsham RH12 SAB, U.K.
Rebecca Butler – Novartis Institutes for Biomedical Research, Horsham Research Center, Horsham RH12 SAB, U.K.
Atwood K. Cheung – Novartis Institutes for Biomedical Research, Cambridge, Massachusetts 02139, United States; orcid.org/0000-0002-2210-6362
Hedaythul Choudhury – Novartis Institutes for Biomedical Research, Horsham Research Center, Horsham RH12 SAB, U.K.
Stephen P. Collingwood – Novartis Institutes for Biomedical Research, Horsham Research Center, Horsham RH12 SAB, U.K.
Brian Cox – Novartis Institutes for Biomedical Research, Horsham Research Center, Horsham RH12 SAB, U.K.; orcid.org/0000-0002-5980-9707
Henry Danahay – Novartis Institutes for Biomedical Research, Horsham Research Center, Horsham RH12 SAB, U.K.
Lee Edwards – Novartis Institutes for Biomedical Research, Horsham Research Center, Horsham RH12 SAB, U.K.; orcid.org/0000-0002-5645-746X
Brian Everatt – Novartis Institutes for Biomedical Research, Horsham Research Center, Horsham RH12 SAB, U.K.
Ulrike Glaenzel – Novartis Institutes for Biomedical Research, Basel CH 4002, Switzerland
Anne-Lise Glotin – Novartis Institutes for Biomedical Research, Horsham Research Center, Horsham RH12 SAB, U.K.
Paul Groot-Kormelink – Novartis Institutes for Biomedical Research, Basel CH 4002, Switzerland
Edward Hall – Novartis Institutes for Biomedical Research, Cambridge, Massachusetts 02139, United States
Julia Hatto – Novartis Institutes for Biomedical Research, Horsham Research Center, Horsham RH12 SAB, U.K.
Catherine Howsham – Novartis Institutes for Biomedical Research, Horsham Research Center, Horsham RH12 SAB, U.K.
Glyn Hughes – Novartis Institutes for Biomedical Research, Horsham Research Center, Horsham RH12 SAB, U.K.
Anna King – Novartis Institutes for Biomedical Research, Horsham Research Center, Horsham RH12 SAB, U.K.
Julia Koehler – Novartis Institutes for Biomedical Research, Basel CH 4002, Switzerland
Swarupa Kulkarni – Novartis Institutes for Biomedical Research, East Hanover, New Jersey 07936, United States
Megan Lightfoot – Novartis Institutes for Biomedical Research, Horsham Research Center, Horsham RH12 SAB, U.K.
Ian Nicholls – Novartis Institutes for Biomedical Research, Basel CH 4002, Switzerland

Christopher Page – Novartis Institutes for Biomedical Research, Horsham Research Center, Horsham RH12 SAB, U.K.

Giles Pergl-Wilson – Novartis Institutes for Biomedical Research, Horsham Research Center, Horsham RH12 SAB, U.K.

Mariana Oana Popa – Novartis Institutes for Biomedical Research, Horsham Research Center, Horsham RH12 SAB, U.K.

Richard Robinson – Novartis Institutes for Biomedical Research, Cambridge, Massachusetts 02139, United States; orcid.org/0000-0002-7209-3424

David Rowlands – Novartis Institutes for Biomedical Research, Cambridge, Massachusetts 02139, United States

Tom Sharp – Novartis Institutes for Biomedical Research, Horsham Research Center, Horsham RH12 SAB, U.K.

Matthew Spendiff – Novartis Institutes for Biomedical Research, Horsham Research Center, Horsham RH12 SAB, U.K.

Emily Stanley – Novartis Institutes for Biomedical Research, Horsham Research Center, Horsham RH12 SAB, U.K.

Oliver Steward – Novartis Institutes for Biomedical Research, Horsham Research Center, Horsham RH12 SAB, U.K.

Roger J. Taylor – Novartis Institutes for Biomedical Research, Horsham Research Center, Horsham RH12 SAB, U.K.

Pamela Tranter – Novartis Institutes for Biomedical Research, Horsham Research Center, Horsham RH12 SAB, U.K.

Trixie Wagner – Novartis Institutes for Biomedical Research, Basel CH 4002, Switzerland

Hazel Watson – Novartis Institutes for Biomedical Research, Horsham Research Center, Horsham RH12 SAB, U.K.

Gareth Williams – Novartis Institutes for Biomedical Research, Basel CH 4002, Switzerland

Penny Wright – Novartis Institutes for Biomedical Research, Horsham Research Center, Horsham RH12 SAB, U.K.

Alice Young – Novartis Institutes for Biomedical Research, Horsham Research Center, Horsham RH12 SAB, U.K.

Complete contact information is available at:

<https://pubs.acs.org/10.1021/acs.jmedchem.1c00343>

Notes

The authors declare the following competing financial interest(s): All authors are former or current employees of Novartis.

■ ACKNOWLEDGMENTS

The authors gratefully acknowledge the following individuals: Dr. Hanna Harant (NIBR Vienna) for generation of the FRT cell lines, Prof Jack Riordan (University of North Carolina Chapel Hill) for provision of the F508del CFTR CHO cell line used for the Quattro assay and Prof Scott Randell (University of North Carolina Chapel Hill) for provision of HBEC.

■ ABBREVIATIONS USED

ALI, air liquid interface; ASL, airway surface liquid; BEGM, bronchial epithelial cell growth medium; CB, chronic bronchitis; CHO, Chinese hamster ovary; COPD, chronic obstructive pulmonary disease; DEA, diethylamine; FLIPR, fluorimetric imaging plate reader; HATU, (1-[bis(dimethylamino)-methylene]-1H-1,2,3-triazolo[4,5-b]pyridinium 3-oxide hexafluorophosphate; LLE, lipophilic ligand efficiency; MCC,

mucociliary clearance; MRT, mean residence time; PoC, proof of concept; SFC, supercritical fluid chromatography

REFERENCES

- (1) About cystic fibrosis. Cystic Fibrosis Foundation: Bethesda, MD, 2017; <https://www.cff.org/What-is-CF/About-Cystic-Fibrosis> (accessed April 1, 2021).
- (2) Riordan, J. R.; Rommens, J. M.; Kerem, R. S.; Alon, N.; Rozmahel, R.; Grzel-czak, Z.; Zielenski, J.; Lok, S.; Plavsic, N.; Chou, J. L.; Drumm, M. L.; Iannuzzi, C.; Collins, F. S.; Tsui, L. C. Identification of the cystic fibrosis gene: cloning and characterization of complementary DNA. *Science* **1989**, *245*, 1066–1073.
- (3) Garland, A. L.; Walton, W. G.; Coakley, R. D.; Tan, C. D.; Gilmore, R. C.; Hobbs, C. A.; Tripathy, A.; Clunes, L. A.; Bencharit, S.; Stutts, M. J.; Betts, L.; Redinbo, M. R.; Tarran, R. Molecular basis for pH-dependent mucosal dehydration in cystic fibrosis airways. *Proc. Natl. Acad. Sci. U. S. A.* **2013**, *110*, 15973–15978.
- (4) Schmidt, B.; Haaf, J.; Leal, T.; Noel, S. Cystic fibrosis transmembrane conductance regulator modulators in cystic fibrosis: current perspectives. *Clin. Pharmacol.: Adv. Appl.* **2016**, *8*, 127–140.
- (5) Hadida, S.; Van Goor, F.; Zhou, J.; Arumugam, V.; McCartney, J.; Hazlewood, A.; Decker, C.; Negulescu, P.; Grootenhuis, P. D. Discovery of N-(2,4-di-tert-butyl-5-hydroxyphenyl)-4-oxo-1,4-dihydroquinoline-3-carboxamide (VX-770, ivacaftor), a potent and orally bioavailable CFTR potentiator. *J. Med. Chem.* **2014**, *57*, 9776–9795.
- (6) De Boeck, K. Cystic fibrosis in the year 2020: A disease with a new face. *Acta Paediatr.* **2020**, *109*, 893–899.
- (7) Ridley, K.; Condren, M. Elexacaftor-Tezacaftor-Ivacaftor: the first triple-combination cystic fibrosis transmembrane conductance regulator modulating therapy. *J. Pediatr. Pharmacol. Ther.* **2020**, *25*, 192–197.
- (8) Van der Plas, S. E.; Kelgtermans, H.; De Munck, T.; Martina, S. L. X.; Dropsit, S.; Quinton, E.; De Blicke, A.; Joannes, C.; Tomaskovic, L.; Jans, M.; Christophe, T.; van der Aar, E.; Borgonovi, M.; Nelles, L.; Gees, M.; Stouten, P.; Van Der Schueren, J.; Mammoliti, O.; Conrath, K.; Andrews, M. Discovery of N-(3-Carbamoyl-5,5,7,7-tetramethyl-5,7-dihydro-4H-thieno[2,3-c]pyran-2-yl)-1H-pyrazole-5-carboxamide (GLPG1837), a novel potentiator which can open class III mutant cystic fibrosis transmembrane conductance regulator (CFTR) channels to a high extent. *J. Med. Chem.* **2018**, *61*, 1425–1435.
- (9) Van der Plas, S. E.; Kelgtermans, H.; Mammoliti, O.; Menet, C.; Tricarico, G.; De Blicke, A.; Joannes, C.; De Munck, T.; Lambin, D.; Cowart, M.; Dropsit, S.; Martina, S. L. X.; Gees, M.; Wesse, A.-S.; Conrath, K.; Andrews, M. Discovery of GLPG2451, a novel once daily potentiator for the treatment of cystic fibrosis. *J. Med. Chem.* **2021**, *64*, 343–351.
- (10) Spanò, V.; Venturini, A.; Genovese, M.; Barreca, M.; Raimondi, M. V.; Montalbano, A.; Galletta, L. J. V.; Barraja, P. Current development of CFTR potentiators in the last decade. *Eur. J. Med. Chem.* **2020**, *204*, 112631.
- (11) World Health Organization website: www.who.int/news-room/fact-sheets/detail/the-top-10-causes-of-death (accessed April 1, 2021).
- (12) Global initiative for chronic obstructive lung disease. *Global strategy for the diagnosis, management, and prevention of chronic obstructive pulmonary disease (2020 report)*. <https://goldcopd.org/gold-reports/> (accessed April 1, 2021).
- (13) World Health Organization fact sheets: Chronic obstructive pulmonary disease [https://www.who.int/news-room/fact-sheets/detail/chronic-obstructive-pulmonary-disease-\(copd\)](https://www.who.int/news-room/fact-sheets/detail/chronic-obstructive-pulmonary-disease-(copd)) (accessed April 1, 2021).
- (14) Hogg, J. C.; Chu, F.; Utokaparch, S.; Woods, R.; Elliott, W. M.; Buzatu, L.; Cherniack, R. M.; Rogers, R. M.; Sciurba, F. C.; Coxson, H. O.; Pare, P. D. The nature of small-airway obstruction in chronic obstructive pulmonary disease. *N. Engl. J. Med.* **2004**, *350*, 2645–2653.
- (15) Kim, V.; Kelemen, S. E.; Abuel-Haija, M.; Gaughan, J. P.; Sharafkaneh, A.; Evans, C. M.; Dickey, B. F.; Solomides, C. C.; Rogers, T. J.; Criner, G. J. Small airway mucous metaplasia and inflammation in chronic obstructive pulmonary disease. *COPD* **2008**, *5*, 329–338.
- (16) McDonough, J. E.; Yuan, R.; Suzuki, M.; Seyednejad, N.; Elliott, W. M.; Sanchez, P. G.; Wright, A. C.; Geffer, W. B.; Litzky, L.; Coxson, H. O.; Pare, P. D.; Sin, D. D.; Pierce, R. A.; Woods, J. C.; McWilliams, A. M.; Mayo, J. R.; Lam, S. C.; Cooper, J. D.; Hogg, J. C. Small-airway obstruction and emphysema in chronic obstructive pulmonary disease. *N. Engl. J. Med.* **2011**, *365*, 1567–1575.
- (17) Fahy, J. V.; Dickey, B. F. Airway mucus function and dysfunction. *N. Engl. J. Med.* **2010**, *363*, 2233–2247.
- (18) Guerra, S.; Sherrill, D. L.; Venker, C.; Ceccato, C. M.; Halonen, M.; Martinez, F. D. Chronic bronchitis before age 50 years predicts incident airflow limitation and mortality risk. *Thorax* **2009**, *64*, 894–900.
- (19) Kim, V.; Zhao, H.; Boriek, A. M.; Anzueto, A.; Soler, X.; Bhatt, S. P.; Rennard, S. I.; Wise, R.; Comellas, A.; Ramsdell, J. W.; Kinney, G. L.; Han, M. K.; Martinez, C. H.; Yen, A.; Black-Shinn, J.; Porszasz, J.; Criner, G. J.; Hanania, N. A.; Sharafkaneh, A.; Crapo, J. D.; Make, B. J.; Silverman, E. K.; Curtis, J. L. Persistent and newly developed chronic bronchitis are associated with worse outcomes in chronic obstructive pulmonary disease. *Ann. Am. Thorac. Soc.* **2016**, *13*, 1016–1025.
- (20) Kesimer, M.; Smith, B. M.; Ceppe, A.; Ford, A. A.; Anderson, W. H.; Barr, R. G.; O'Neal, W. K.; Boucher, R. C.; Woodruff, P. G.; Han, M. K.; Hoffman, E. A.; Martinez, F.; Curtis, J. L.; Paine, R.; Cooper, C. B.; Bleeker, E. R. Mucin concentrations and peripheral airways obstruction in COPD. *Am. J. Respir. Crit. Care Med.* **2018**, *198*, 1453–1456.
- (21) Kesimer, M.; Ford, A. A.; Ceppe, A.; Radicioni, G.; Cao, R.; Davis, C. W.; Doerschuk, C. M.; Alexis, N. E.; Anderson, W. H.; Henderson, A. G.; Barr, R. G.; Bleeker, E. R.; Christenson, S. A.; Cooper, C. B.; Han, M. K.; Hansel, N. N.; Hastie, A. T.; Hoffman, E. A.; Kanner, R. E.; Martinez, F.; Paine, R., 3rd; Woodruff, P. G.; O'Neal, W. K.; Boucher, R. C. Airway mucin concentration as a marker of chronic bronchitis. *N. Engl. J. Med.* **2017**, *377*, 911–922.
- (22) Cantin, A. M.; Hanrahan, J. W.; Bilodeau, G.; Ellis, L.; Dupuis, A.; Liao, J.; Zielenski, J.; Durie, P. Cystic fibrosis transmembrane conductance regulator function is suppressed in cigarette smokers. *Am. J. Respir. Crit. Care Med.* **2006**, *173*, 1139–1144.
- (23) Clunes, L. A.; Davies, C. M.; Coakley, R. D.; Aleksandrov, A. A.; Henderson, A. G.; Zeman, K. L.; Worthington, E. N.; Gentzsch, M.; Kreda, S. M.; Cholon, D.; Bennett, W. D.; Riordan, J. R.; Boucher, R. C.; Tarran, R. Cigarette smoke exposure induces CFTR internalization and insolubility, leading to airway surface liquid dehydration. *FASEB J.* **2012**, *26*, 533–545.
- (24) Kreindler, J. L.; Jackson, A. D.; Kemp, P. A.; Bridges, R. J.; Danahay, H. Inhibition of chloride secretion in human bronchial epithelial cells by cigarette smoke extract. *Am. J. Physiol. Lung Cell Mol. Physiol.* **2005**, *288*, L894–902.
- (25) Raju, S. V.; Lin, V. Y.; Liu, L.; McNicholas, C. M.; Karki, S.; Sloane, P. A.; Tang, L.; Jackson, P. L.; Wang, W.; Wilson, L.; Macon, K. J.; Mazur, M.; Kappes, J. C.; DeLucas, L. J.; Barnes, S.; Kirk, K.; Tearney, G. J.; Rowe, S. M. The cystic fibrosis transmembrane conductance regulator potentiator ivacaftor augments mucociliary clearance abrogating cystic fibrosis transmembrane conductance regulator inhibition by cigarette smoke. *Am. J. Respir. Cell Mol. Biol.* **2017**, *56*, 99–108.
- (26) Dransfield, M. T.; Wilhelm, A. M.; Flanagan, B.; Courville, C.; Tidwell, S. L.; Raju, S. V.; Gaggar, A.; Steele, C.; Tang, L. P.; Liu, B.; Rowe, S. M. Acquired cystic fibrosis transmembrane conductance regulator dysfunction in the lower airways in COPD. *Chest* **2013**, *144*, 498–506.
- (27) Raju, S. V.; Jackson, P. L.; Courville, C. A.; McNicholas, C. M.; Sloane, P. A.; Sabbatini, G.; Tidwell, S.; Tang, L. P.; Liu, B.; Fortenberry, J. A.; Jones, C. W.; Boydston, J. A.; Clancy, J. P.; Bowen, L. E.; Accurso, F. J.; Blalock, J. E.; Dransfield, M. T.; Rowe, S. M. Cigarette smoke induces systemic defects in cystic fibrosis transmembrane conductance regulator function. *Am. J. Respir. Crit. Care Med.* **2013**, *188*, 1321–1330.
- (28) Sloane, P. A.; Shastri, S.; Wilhelm, A.; Courville, C.; Tang, L. P.; Backer, K.; Levin, E.; Raju, S. V.; Li, Y.; Mazur, M.; Byan-Parker, S.; Grizzle, W.; Sorscher, E. J.; Dransfield, M. T.; Rowe, S. M. A

pharmacologic approach to acquired cystic fibrosis transmembrane conductance regulator dysfunction in smoking related lung disease. *PLoS One* **2012**, 7, No. e39809.

(29) Courville, C. A.; Tidwell, S.; Liu, B.; Accurso, F. J.; Dransfield, M. T.; Rowe, S. M. Acquired defects in CFTR-dependent beta-adrenergic sweat secretion in chronic obstructive pulmonary disease. *Respir. Res.* **2014**, 15, 25.

(30) Lambert, J. A.; Raju, S. V.; Tang, L. P.; McNicholas, C. M.; Li, Y.; Courville, C. A.; Farris, R. F.; Coricor, G. E.; Smoot, L. H.; Mazur, M. M.; Dransfield, M. T.; Bolger, G. B.; Rowe, S. M. Cystic fibrosis transmembrane conductance regulator activation by roflumilast contributes to therapeutic benefit in chronic bronchitis. *Am. J. Respir. Cell Mol. Biol.* **2014**, 50, 549–558.

(31) Solomon, G. M.; Hathorne, H.; Liu, B.; Raju, S. V.; Reeves, G.; Acosta, E. P.; Dransfield, M. T.; Rowe, S. M. Pilot evaluation of ivacaftor for chronic bronchitis. *Lancet Resp. Med.* **2016**, 4, e32–e33.

(32) Hwang, T. C.; Wang, F.; Yang, I. C.; Reenstra, W. W. Genistein potentiates wild-type and delta F508-CFTR channel activity. *Am. J. Physiol.* **1997**, 273, C988–998.

(33) Pedemonte, N.; Sonawane, N. D.; Taddei, A.; Hu, J.; Zegarar-Moran, O.; Suen, Y. F.; Robins, L. I.; Dicus, C. W.; Willenbring, D.; Nantz, M. H.; Kurth, M. J.; Galletta, L. J.; Verkman, A. S. Phenylglycine and sulfonamide correctors of defective delta F508 and G551D cystic fibrosis transmembrane conductance regulator chloride-channel gating. *Mol. Pharmacol.* **2005**, 67, 1797–1807.

(34) Baxter, D. F.; Kirk, M.; Garcia, A. F.; Raimondi, A.; Holmqvist, M. H.; Flint, K. K.; Bojanic, D.; Distefano, P. S.; Curtis, R.; Xie, Y. A novel membrane potential-sensitive fluorescent dye improves cell-based assays for ion channels. *J. Biomol. Screening* **2002**, 7, 79–85.

(35) Yang, H.; Shelat, A. A.; Guy, R. K.; Gopinath, V. S.; Ma, T.; Du, K.; Lukacs, G. L.; Taddei, A.; Folli, C.; Pedemonte, N.; Galletta, L. J.; Verkman, A. S. Nanomolar affinity small molecule correctors of defective delta F508-CFTR chloride channel gating. *J. Biol. Chem.* **2003**, 278, 35079–35085.

(36) Seifried, H. E.; Seifried, R. M.; Clarke, J. J.; Junghans, T. B.; San, R. H. A compilation of two decades of mutagenicity test results with the Ames salmonella typhimurium and L5178Y mouse lymphoma cell mutation assays. *Chem. Res. Toxicol.* **2006**, 19, 627–644.

(37) Hopkins, A. L.; Keserü, G. M.; Leeson, P. D.; Rees, D. C.; Reynolds, C. H. The role of ligand efficiency metrics in drug discovery. *Nat. Rev. Drug Discovery* **2014**, 13, 105–121.

(38) Peterson, L. A. Reactive metabolites in the biotransformation of molecules containing a furan ring. *Chem. Res. Toxicol.* **2013**, 26, 6–25.

(39) Dahal, U. P.; Obach, R. S.; Gilbert, A. M. Benchmarking in vitro covalent binding burden as a tool to assess potential toxicity caused by nonspecific covalent binding of covalent drugs. *Chem. Res. Toxicol.* **2013**, 26, 1739–1745.

(40) Waldmann, R.; Champigny, G.; Bassilana, F.; Voilley, N.; Lazdunski, M. Molecular cloning and functional expression of a novel amiloride-sensitive Na⁺ channel. *J. Biol. Chem.* **1995**, 270, 27411–27414.

(41) Moran, O.; Zegarar-Moran, O. On the measurement of the functional properties of the CFTR. *J. Cystic Fibrosis* **2008**, 7, 483–494.

(42) Ma, T.; Thiagarajah, J. R.; Yang, H.; Sonawane, N. D.; Folli, C.; Galletta, L. J.; Verkman, A. S. Thiazolidinone CFTR inhibitor identified by high-throughput screening blocks cholera toxin-induced intestinal fluid secretion. *J. Clin. Invest.* **2002**, 110, 1651–1658.

(43) Davies, B.; Morris, T. Physiological parameters in laboratory animals and humans. *Pharm. Res.* **1993**, 10, 1093–1095.

(44) Kazani, S.; Rowlands, D. J.; Bottoli, I.; Milojevic, J.; Alcantara, J.; Jones, I.; Kulmatycki, K.; Machineni, S.; Mostov, L.; Nicholls, I.; Nick, J. A.; Rowe, S. M.; Simmonds, N. J.; Vegesna, R.; Verheijen, J.; Danahay, H.; Gosling, M.; Ayalavajjala, P. S.; Salman, M.; Strieter, R. Safety and efficacy of the cystic fibrosis transmembrane conductance regulator potentiator icenticaftor (QBW251). *J. Cystic Fibrosis* **2021**, 20, 250.

(45) Flume, P. A.; Liou, T. G.; Borowitz, D. S.; Li, H.; Yen, K.; Ordoñez, C. L.; Geller, D. E. Ivacaftor in subjects with cystic fibrosis who are homozygous for the F508del-CFTR mutation. *Chest* **2012**, 142, 718–724.

(46) Rowe, S. M.; Jones, I.; Dransfield, M. T.; Haque, N.; Gleason, S.; Hayes, K. A.; Kulmatycki, K.; Yates, D. P.; Danahay, H.; Gosling, M.; Rowlands, D. J.; Grant, S. S. Efficacy and safety of the CFTR potentiator icenticaftor (QBW251) in COPD: results from a phase 2 randomized trial. *Int. J. Chronic Obstruct. Pulm. Dis.* **2020**, 15, 2399–2409.

(47) Duvoix, A.; Dickens, J.; Haq, I.; Mannino, D.; Miller, B.; Tal-Singer, R.; Lomas, D. A. Blood fibrinogen as a biomarker of chronic obstructive pulmonary disease. *Thorax* **2013**, 68, 670–676.

(48) ClinicalTrials.gov Identifier: NCT04072887 <https://clinicaltrials.gov/ct2/show/NCT04072887?term=QBW251&draw=2&rank=2> (accessed April 1, 2021).

(49) Heinz, T.; Martin, B.; Rampf, F.; Zaug, W. New picolinic acid derivatives and their use as intermediates. PCT application WO 2018116139, June 28 2018.

(50) Coote, K. J.; Paisley, D.; Czarnecki, S.; Tweed, M.; Watson, H.; Young, A.; Sugar, R.; Vyas, M.; Smith, N. J.; Baettig, U.; Groot-Kormelink, P. J.; Gosling, M.; Lock, R.; Ethell, B.; Williams, G.; Schumacher, A.; Harris, J.; Abraham, W. M.; Sabater, J.; Poll, C. T.; Faller, T.; Collingwood, S. P.; Danahay, H. NVP-QBE170: an inhaled blocker of the epithelial sodium channel with a reduced potential to induce hyperkalaemia. *Br. J. Pharmacol.* **2015**, 172, 2814–2826.

(51) Cheung, A. K.; Hurley, B.; Kerrigan, R.; Shu, L.; Chin, D. N.; Shen, Y.; O'Brien, G.; Sung, M. J.; Hou, Y.; Axford, J.; Cody, E.; Sun, R.; Fazal, A.; Fridrich, C.; Sanchez, C. C.; Tomlinson, R. C.; Jain, M.; Deng, L.; Hoffmaster, K.; Song, C.; Van Hoosear, M.; Shin, Y.; Servais, R.; Towler, C.; Hild, M.; Curtis, D.; Dietrich, W. F.; Hamann, L. G.; Briner, K.; Chen, K. S.; Kobayashi, D.; Sivasankaran, R.; Dales, N. A. Discovery of small molecule splicing modulators of survival motor neuron-2 (SMN2) for the Treatment of Spinal Muscular Atrophy (SMA). *J. Med. Chem.* **2018**, 61, 11021–11036.